Advanced Course on

Photometry and Spectroscopy at the 80 cm telescope

Thomas Schanz

The German version of this experiment manual was created by Thorsten Nagel in the years 2004 to 2008 based on earlier manuals for a CCD-camera experiment and experimental physics labwork by Jörn Wilms, Stefan Dreizler, Ralf Geckeler, and Martin Bässgen, comments of Jochen L. Deetjen and Lisa Löbling, and the scientific work of Margit Haberreiter1. The manual had been maintained by Cornelia Heinitz from 2015 to 2017 and Thomas Rauch from 2017 to 2023. Since then, Thomas Schanz is responsible.

Contents

1 The Experiment

This experiment presents the 80 cm telescope of the IAAT and two major applications of astronomy: Photometry and Spectroscopy. Photometry is measuring the brightness of stars. In this course it is used to determine the distance and age of open star clusters. In Spectroscopy, the spectrum of light is measured. The occurrence of absorption lines in the spectrum permits the detection of chemical elements that are present in the atmospheres of stars. If the weather conditions (seeing) permits, we will exposure a CCD image of an open star cluster for photometry and record the spectrum of a star utilizing the spectrograph of the IAAT. If the sky is obscured by clouds at the course day, we will still presenting the 80 cm telescope and its operation in a simulated observation and provide photographic and spectroscopic data from some former observations for analysis.

Figure 1 shows the 80 cm telescope inside the 5 meter dome of the IAAT observatory.
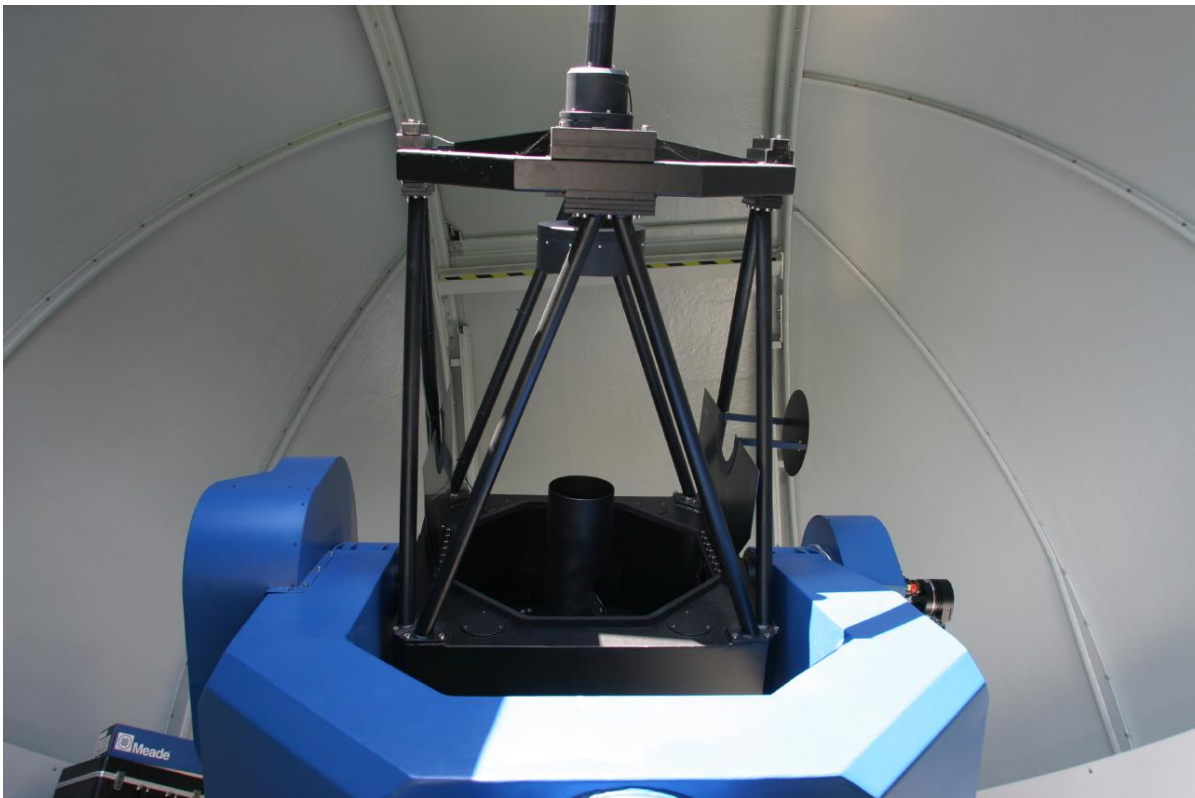

Figure 1: The 80 cm mirror telescope of the IAAT

The exercises you will find in this guide are part of the course and are expected to be discussed in the protocol as well.

2 Motivation

Astronomy is the science of all objects and phenomena beyond Earths atmosphere above a height of 100 km over sea level. Space flight gave humans physical access to some nearby objects inside the solar systems, like Earth moon and some scattered asteroids. Just recently, scientists witnessed the dawn of two new fields of astronomy, neutrino- and gravitational wave astronomy. Besides this exceptions, any information and data that have ever been collected by astronomers over the centuries were transported by light, or more general, by electromagnetic waves that have carried these informations from extraterrestrial sources to the instrumentation of scientists on Earth.

When asking, how information can be carried by light-waves through the vacuum of space, there are 4 possible answers:

a.) **'Positioning'** and **'Imaging'** - the angular information:
'Positioning' is probably the oldest technique in astronomy. The positioning of the stars goes back to Hipparchus who mapped the position of about 900 stars at 100 BC. The technique that is mapping the angular information is called: 'Imaging'. 'Imaging' was restricted to the naked eye before the invention of the telescope by Galileo Galilei (1608) and Johannes Kepler (1611). Besides the moon and the sun, astronomical objects are much to small in angular distribution in order to see an actual image of the object. Curiously, what humans see in that case, is just the response function of the optical system, the point spread function (PSF) of the human eye. That's the reason why most objects just look alike at the night sky, anyway if its a far away sun, a planet, or an orbiting spacecraft. Before the invention of the telescope, 'Imaging' did basically not exist, astronomy was limited to 'Positioning'. With the invention of the telescope the situation changed, at least for nearby objects and for objects with extraordinary large angular distribution. A huge progress for 'Imaging' was the invention of 'Photography' by Louis Daguerre (1839) that made observations more persistent and objective. From there on, astronomical photographs could be stored and published, they also could be analyzed and discussed by a larger community of scientists. Photography also allowed long time exposure for the very first time, revealing very faint objects that nobody had ever seen before. Today, 'Imaging' is based on digital photography, the electronic cameras make use of CCD[1] light sensors, invented by Willard Boyle and George Smith (1969) and their successors, so called Active-Pixel-Sensors (APS). Images can be recorded in a high rate with high spatial resolution. Their data can be corrected and processed in real-time by computers and transferred by radio signals easily from space telescopes in Earth orbit or from distant space probes millions of miles from Earth away.

---

[1]Charge-Coupled-Device

The instrument for 'Imaging' is the 'Camera', a recording device with spatial resolution. The IAAT owns two digital cameras for use at the 80 cm telescope. There is a 1 Megapixel black and white photometric CCD camera with a filter-wheel, the SBIG STL1001, and a 14 Megapixel MOS video camera for color imaging, the ZWO ASI294 that employs an Active-Pixel-Sensor.

b.) **'Photometry'** - brightness and temporal information:
The brightness of the stars was first mapped by Hipparchus (100 BC), he introduced also the magnitude scale of the stars that is basically still in use today. The brightness of stars depends on their distance from Earth but also on their surface size, temperature and their mass. Stars can be classified by their brightness and their color. A systematic classification of about 500000 stars was first made by Edward Pickering (1884) and Annie Jump-Cannon (1903), later Ejnar Hertzsprung (1905) defined the 'absolute magnitude' of stars and Henry Russel (1913) discovered that stars can be classified in a brightness/color diagram, where the life of the stars can be mapped by their movement through different branches of the 'Hertzsprung-Russel-Diagram' (HRD). From their spectral classification, the absolute magnitude of stars can be determined in the HRD. Using the relative magnitude from local observations, the distance of a particular star can be calculated from the HRD. Stars can also change their brightness over time, pulsating stars (Cepheids) can be used as standard candles since the pulse periods are corresponding to their absolute magnitudes (Henrietta Leavitt, 1912). The technique of recording the brightness of stars and their light curves over time is called 'Photometry' and it became very important for scaling the distance ladder of astronomy.

The instrument for 'Photometry' is a 'Camera' with temporal resolution and a number of selectable color filters on a filter wheel. The IAAT employs a 1 Megapixel black and white CCD camera (SBIG STL1001) with such a filter wheel for 'Photometry' that can be mounted to the focus of the 80 cm telescope.

c.) **'Spectroscopy'** - the spectral information:
The energy of light is coded in colors. 'Spectroscopy' is a technique that disperses light into its colors as discovered the first time by Sir Isaac Newton (1666). A spectrometer can utilize a prism or grating in order to disperse the light. Since the discovery of lines (emission lines and absorption lines) by Joseph v. Fraunhofer (1850), spectroscopy became a standard tool for astronomers to analyze the chemical composition of light sources as well as investigating the media that is in between the stars and the Earth.

The instrument for 'Spectroscopy' is the spectrometer. The IAAT has a classic long slit spectrometer (10C spectrograph) using a reflection grating and employs also an Echelle spectrometer (BACHES), both can be mounted at the left focus of

the 80 cm telescope.

d.) **'Polarimetry'** - the polarization information:
The polarization of light was first discovered by Étienne-Louis Malus (1808), it can be measured by using a polariser, that is a filter that let pass only light with a particular direction of polarization. Most sources emit unpolarised light, that means the polarization oscillates in all directions. But there are sources that emit linear polarised light of a certain orientation. Unpolarised light can become polarised when scattered on dust particles. Polarimetry can be used to detect dust in protoplanetary discs of stars or in the atmosphere of exoplanets. Also the presence of electric or magnetic fields at the source can be investigated by the polarization of light. Polarization is used to study the expanding debries of supernovae. When the material cloud ejected by a supernova is perfectly spherical in shape, the light is canceling out any polarization, when the ejecta is asymmetric in shape, the light will have a degree of polarization. Polarimetry can be used to measure if a supernova has exploded spherically.

3 Telescopes

The telescope is certainly the most important invention for astronomy. Basically, there are two major types of telescopes in existence, 1) the lens telescope or *'refractor'*, 2) the mirror telescope or *'reflector'*. Common for both types of telescopes is the collection of light from a certain direction and the magnification of angular information. Figure 2 shows the optical light path for a refracting and for a reflecting telescope.
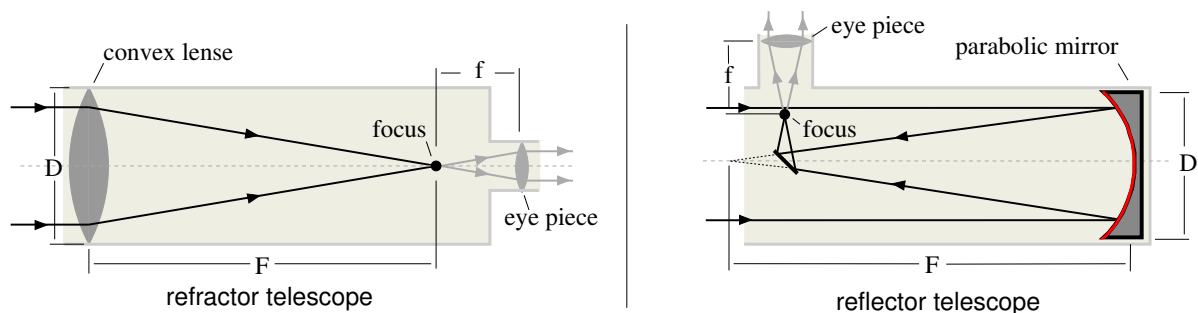
Figure 2: The two types of telescopes: lens telescope (left), mirror telescope (right)

Both types of telescopes have similar physical parameters. The amount of light the telescope can gather is determined by the aperture 'D', that is either the diameter of the objective lens of the refracting telescope or the size of the parabolic mirror in case of the reflecting telescope. The ratio between 'D' and the focal length 'F', (D/F) is called

'aperture ratio' and a measure for the brightness of the optical system. A telescope with a higher 'aperture ratio' will produce a brighter image at the same aperture 'D' compared to a telescope with a lower 'aperture ratio'. The magnification of the telescope is given by the ratio 'F/f' between the focal length of the main lens/mirror 'F' and the focal length of the eye piece 'f'.

The resolving power of a telescope is defined by the ability of the telescope to distinguish clearly two objects. This resolving power however is limited by the diffraction of the star light at the aperture of the telescope optic. The intensity distribution $I(\Theta)$ for a circular aperture of radius 'r' is given by Equation 1:

$$I_\Theta \propto \frac{\pi^2 r^4}{m^2}(J_1(2m))^2 \tag{1}$$

with

$$m = \frac{\pi r \sin\Theta}{\lambda} \tag{2}$$

$J_1(2m)$ is the first order Bessel function of the first kind. Figure 3 (left) shows a graph of the Bessel function $J_1(2m)/m$. The intensity is zero in concentric rings of radius Θ:

$$\Theta \approx \frac{1.220\lambda}{D}, \quad \frac{2.233\lambda}{D}, \quad \frac{3.238\lambda}{D}, ... \tag{3}$$

where D = 2r is the diameter of the telescope aperture. Figure 3 (right) shows the diffraction of an object. The inner part of the disc is called 'Airy' disc, after the astronomer 'George B. Airy' who derived Equation 1 the very first time. Figure 3 (right) shows the photograph of such an 'Airy' disc. The light of a star, will produce an extended disc of radius $1.22\lambda/D$ surrounded by diffraction rings at the telescope.

In order to characterize the resolution of a telescope the criteria of Lord Rayleigh is used. Two equally bright objects can be distinguished from each other when the intensity maximum of the diffraction disc of the first object falls onto the first intensity minimum of the diffraction disc of the second. For the theoretical resolution 'α' of the telescope follows Equation 4:

$$\alpha = 1.220_{rad} \frac{\lambda}{D} \approx 70° \frac{\lambda}{D} \tag{4}$$
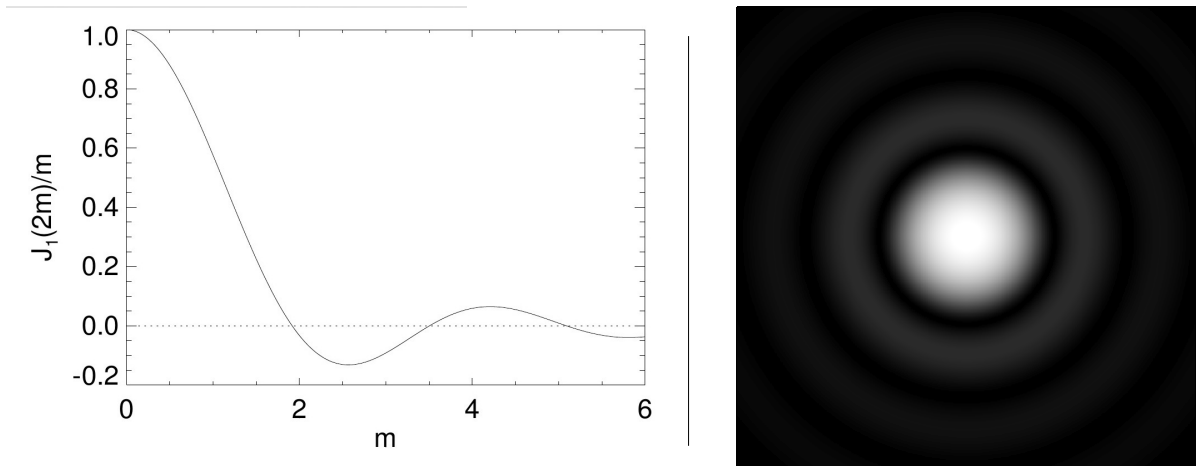
Figure 3: left: Function $J_1(2m)/m$, the square of $J_1(2m)/m$ describes the intensity distribution of a circular aperture. right: photograph of an diffraction image.

Unfortunately this theoretical resolution can never be reached. The Earth atmosphere is limiting the resolution of the telescope severely by turbulences and waveform distortions. For any practical use, the best resolution that can be reached is limited to $\alpha \approx \lambda/D$.

<div style="text-align:center; color:blue">

Exercise 1: Calculate the theoretical resolution (in arc seconds) of a telescope with an aperture of 80 cm at a wavelength of 5700 Å.

</div>

3.1 Coordinate systems

In order to locate an object in the sky, a definite coordinate system is required that is independent from the observation site on Earth and the time. Such a coordinate system can be defined on an infinite large celestial sphere. Since the distance to the stars is so large (the next star, Proxima Centauri, has a distance of about 270000 AU), the daily or yearly movement of Earth is insignificantly small and can be neglected.

Figure 4 shows the commonly used coordinate system (declination / right ascension) in astronomy. The red lines define the local azimutal coordinate system at the site of the observer with the observer in the center. Notice the cardinal points for East 'E', South 'S', West 'W' and North 'N' and the red line for the local horizon. Since the celestial coordinate system shall be independent from the observation site it is rather attached to the rotation axis of Earth that is shown by the green lines. The rotation axis extends through the 'celestial north pole' and 'celestial south pole', the celestial north pole is pointing almost precisely in direction of the star 'Polaris' in constellation 'Ursa Minor'. In right angle to the celestial north-south-pole axis is a plane that is called the 'celestial equator', an intersection of the celestial sphere with Earth's equator plane. The angular
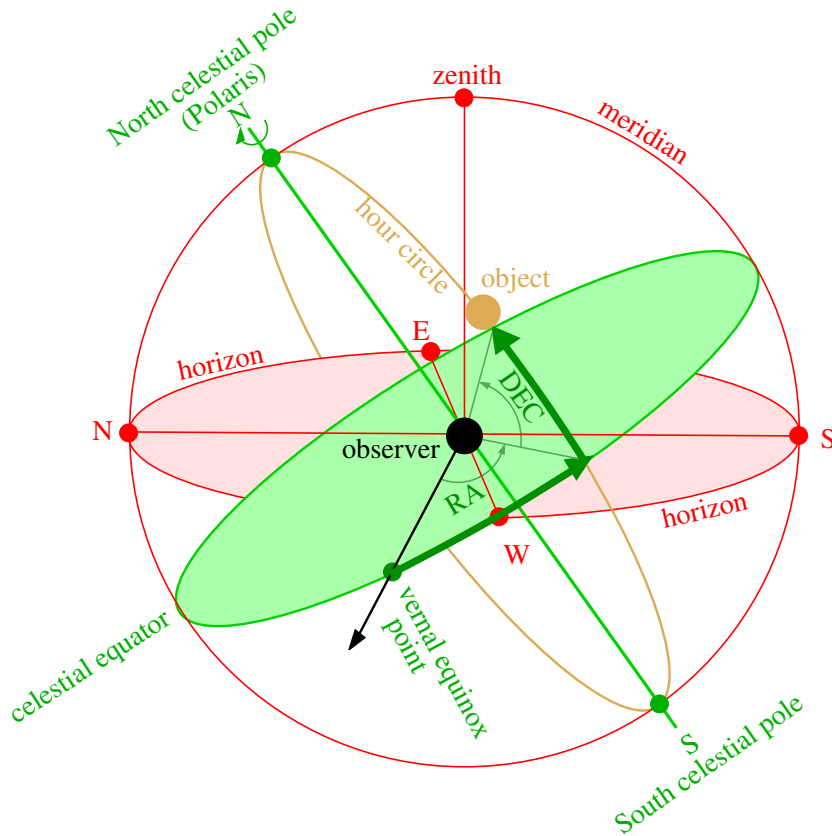
9

Figure 4: Celestial sphere with coordinates

distance of an celestial objects from the celestial equator plane is independent from the rotation of Earth and measured on a circle that goes through both celestial poles and the celestial objects location. The circle is called the 'hour circle' (orange line) and the angular distance of the celestial object measured from the celestial equator is named **'declination'** (DEC). Objects in the northern hemisphere have positive declination angles while objects in the southern hemisphere have negative declination angles. DEC is measured in 'degrees', 'arc-minutes' and 'arc-seconds'.

The second coordinate is called **'right ascension'** (RA) and is depending on the rotation of Earth. Therefore, RA is measured in 'hours', 'minutes' and 'seconds' relative to a reference point.

> Exercise 2: Consult the SIMBAD (http://simbad.u-strasbg.fr/simbad) web data base and note the celestial coordinates (R.A. in [HH:MM:SS], DEC in [Deg:Min:Sec]) for all objects in Table 3. Set up an observation schedule using the coordinates of the object list for the observation night, which objects can be observed best at what local time?

3.2 The 80 cm telescope

The Observatory of the IAAT at Sand was build and commissioned in the year 2003. It is using a mirror telescope in Cassegrain configuration with Nasmyth focus, a main mirror size 'D' of 80 cm diameter and a focal length 'F' of 6.4 meters. The telescope is mounted on an equatorial open fork mount for slewing and automatic tracking of astronomical objects over the sky. The equatorial mount requires only the tracking of one single axis in order to compensate the rotation of Earth. All operations of the observatory are fully computer controlled.
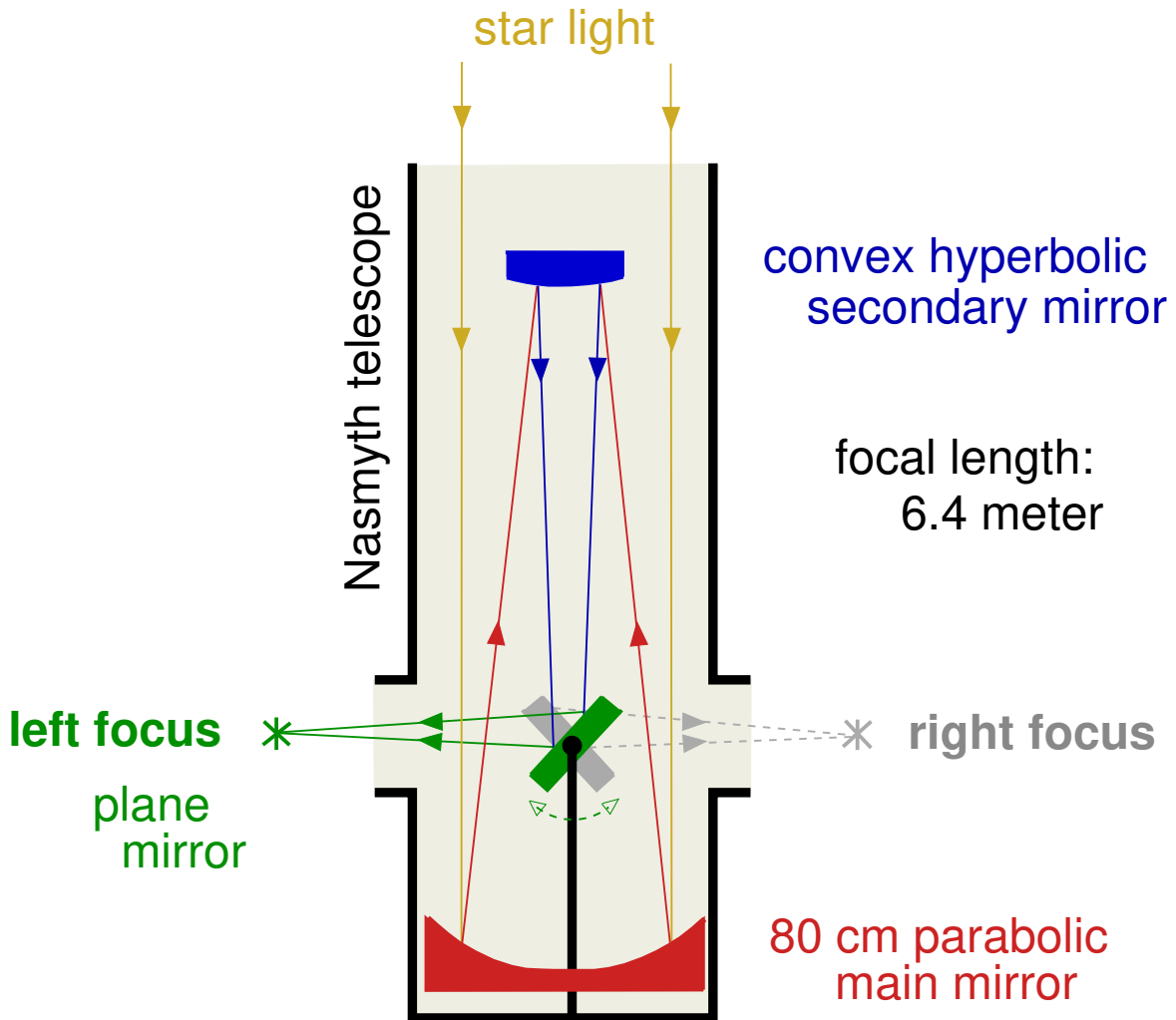
Figure 5: light path of the 80 cm mirror telescope

The optical beam path of the telescope is shown in Figure 5. The starlight will enter from above and be reflected by the 80 cm main mirror onto the secondary mirror that is about 2 meters above the main mirror. From there on, the light is further focused

and reflected back onto a plane mirror that is mounted inside a hole of the main mirror, it will reflect the light out of the telescope along the declination axis of the telescope. The main mirror is parabolic, the secondary mirror hyperbolic. The plane mirror can be rotated by a motor to exit the light either to the left focus or to the right focus of the telescope. Such a 'Nasmyth' configuration allows the mounting of heavy cameras or spectroscopic equipment to the telescope that does not need to be moved with the declination axis. The Cassegrain-Nasmyth configuration is folding the light-path and allows a very compact setup of the telescope. With a focal length of over 6 meter, the length of the telescope tube is only about 3 meters long.

Figure 6 shows a compare between three mirror telescope types that all have a focal length of 6.4 meter. While the Newton type telescope has a tubus length of 6 meter, the Cassegrain and the Nasmyth types are much more compact. The Nasmyth configuration is only 3 meter long and would require merely a dome size of 5 meter diameter for operation. The Cassegrain and Nasmyth telescope types are also very popular for portable telescopes due to their compactness.

> Exercise 3: What is the angular velocity for the telescope to compensate the Earth's rotation? Use a year length of 365.25 days. How long is a stellar day?
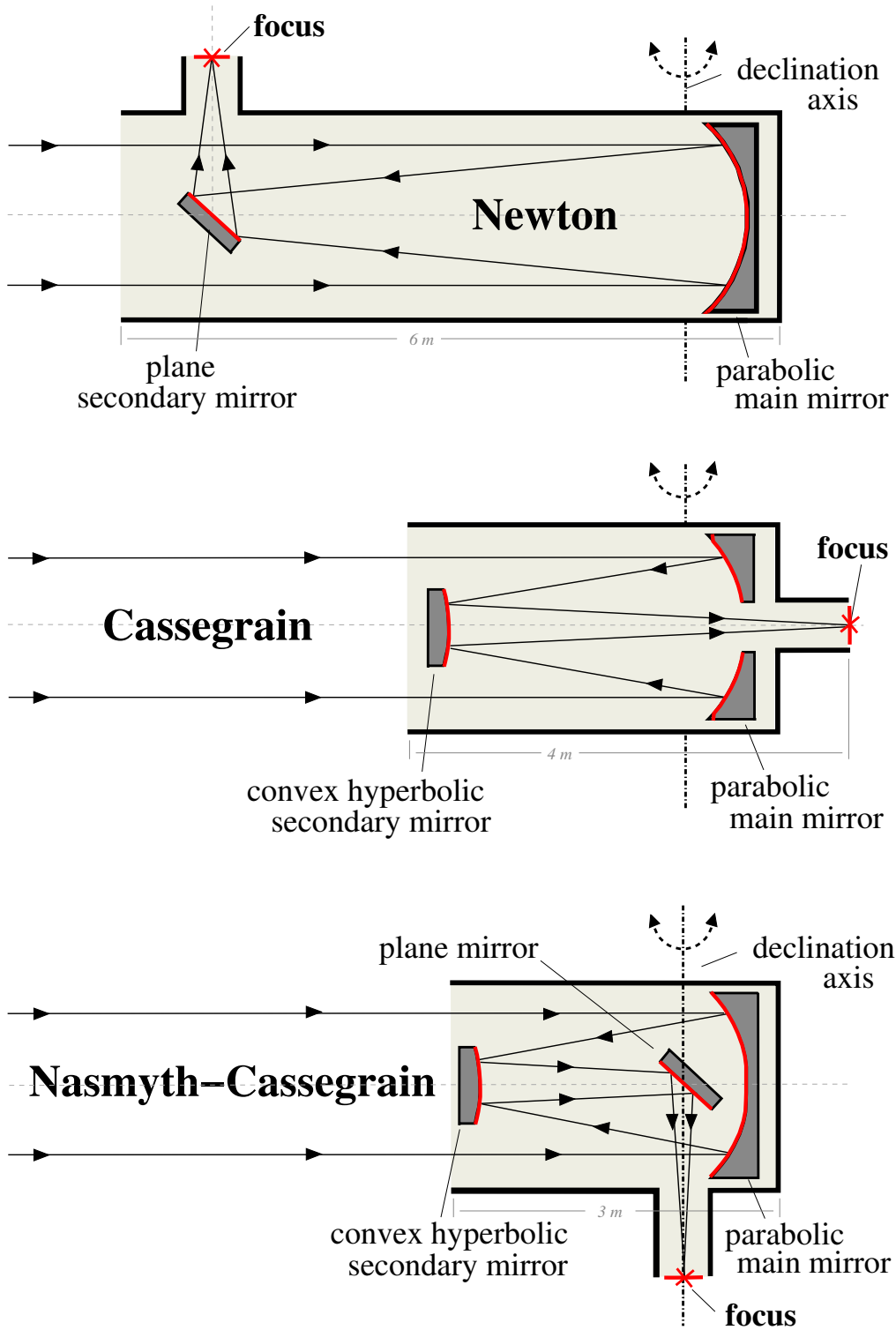
Figure 6: Compare of three different mirror telescope types with the same focal length of 6.4 meter. The Nasmyth telescope has by far the most compact setup at about 3 meter length, while the Newton tubus will be almost 6 meter long.

13

4 Cameras

CCD Cameras are electronic cameras that make use of 'Charge-Couple-Device' (CCD) semiconductor sensors. The semiconductor crystal of such a sensor is structured in millions of small compartments, called 'Pixels'. Photons that enter the crystal are interacting by the 'Photo-electric-effect', generating clouds of electric charges near the location of the interaction which will than be stored inside the pixels. An external electrical biasing of the CCD is confining the generated charges inside the pixels until further readout. Therefore, the sensor is recording the spatial information of photon interactions, resulting in an 'Image' of the light source.
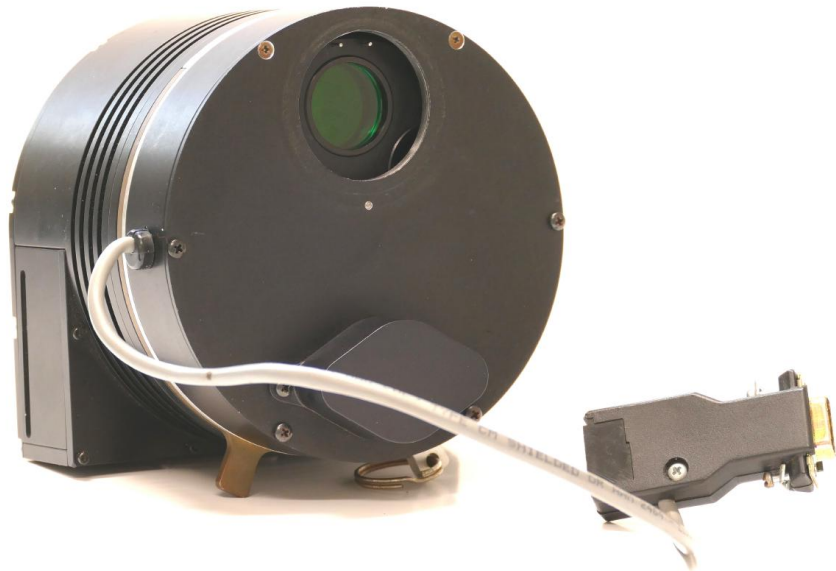
Figure 7: Typical astronomical camera that is using a CCD light sensitive sensor. The CCD can only record a black and white image with graded shades of gray. In order to generate a colored image, three images with filters for 'red', 'green' and 'blue' light must be recorded and stagged together into a color image by software later.

4.1 Photo electric effect

Considering the interaction of radiation with matter, the photo electric effect is the dominant effect for energies at the range of optical light. A photon that enters the crystal will transfer its complete energy onto a single electron, called a 'photo-electron'

14

(pe). Is the transferred energy larger than the binding-energy of the electron to the valence-band of the semiconductor, the 'pe' will leave the valence-band and enter the conduction-band or it collides with other electrons of the valence-band while lifting them into the conduction-band. For each electron that enters the conduction-band, a hole is created in the valence-band. The thereby generated electron-hole-pairs will increase the electric conductivity of the semiconductor and will lead to an electric current that can be measured. Figure 8 gives an illustration of the photo-electric-effect on basis of the band model for semiconductors.
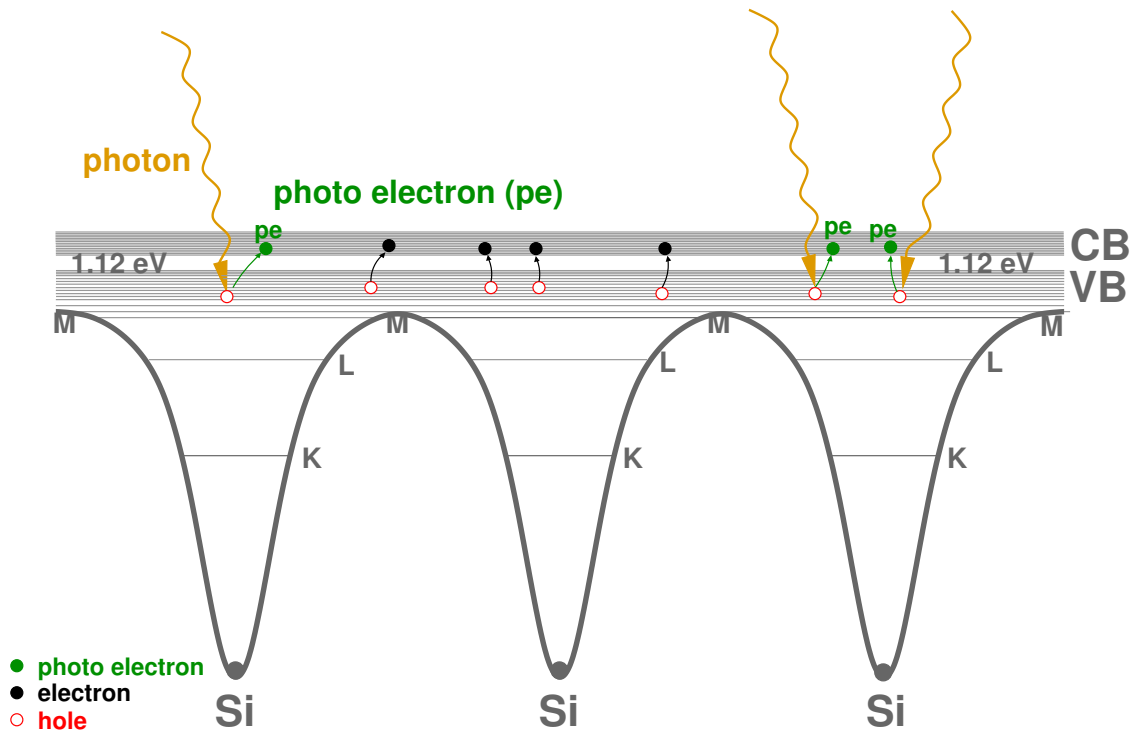

Figure 8: The interaction of photons with the semiconductor by photo-electric-effect. A photon is transferring its energy onto a photo-electron (pe) (green) that will be lifted up from the valence-band (VB) into the conduction-band (CB) of the semiconductor.

Figure 8 shows the band model of the silicon semiconductor crystal and the interaction of photons by the photo-electric-effect. Unfortunately there is a large number of electron-hole-pairs also be generated by thermal excitations, leading to a severe dark-current that is always present even without any photon interactions and superimposed to the recorded photonic signals. Silicon has a band gap of 1.12 eV between valence band and conduction band. The dark-current of the semiconductor can be reduced by cooling. It can also be compensated by generating and using an offset-map. The offset-map is made from a dark-image, where the sensor is shielded from light and only recording the thermal induced dark-current that is constant for individual pixels in average over time. The offset-map is stored inside the camera and subtracted from all exposured images of

the sensor, removing the majority of the thermal generated background signals.

> Exercise 4: Estimate how many electrons per photon are generated inside a silicon semiconductor when a photon of $\lambda = 4686$ Å hits the Si semiconductor? Why is it impossible to use a Si semiconductor as a sensor for infrared radiation in the K band of $\lambda = 2.2$ μm?

4.2 The Photo-Diode

The basic element of the CCD is the 'Photo-Diode'. A Photo-Diode is made of two doped semiconductors, an n-doped semiconductor that has a surplus of 'electrons' and a p-doped semiconductor that has a surplus of 'holes', directly in contact to each other. At the junction of the n-doped- (n-zone), and p-doped- (p-zone) semiconductors, the surplus electrons of the n-zone will diffuse into the p-zone, leaving a charge free area, called a depletion-zone. Figure 9 gives a cross section of such a pn-Photo-Diode.
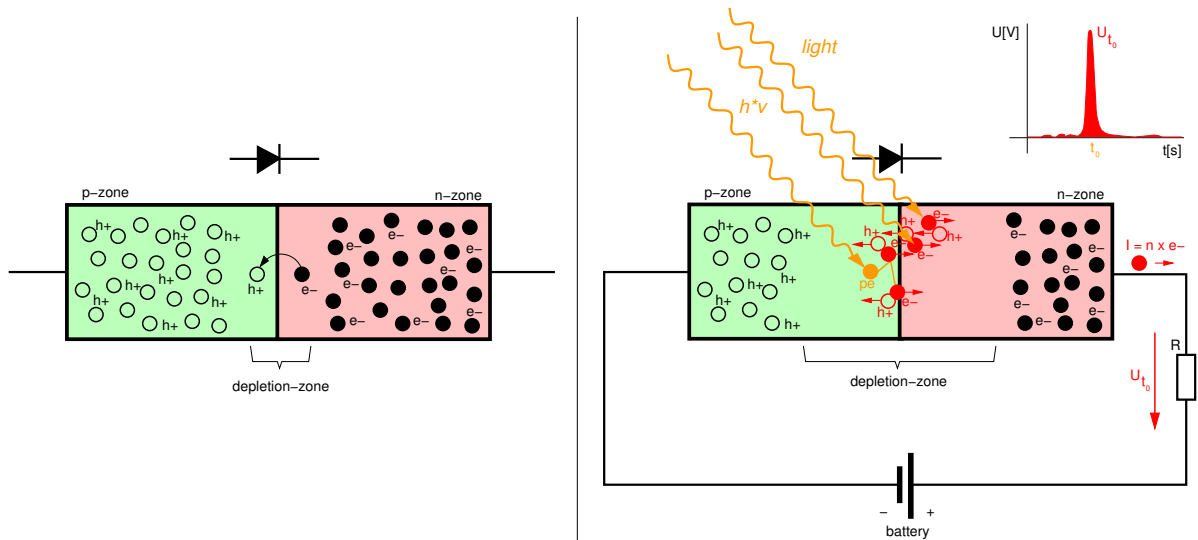
Figure 9: left: Photo-Diode internal setup, **right:** Photo-Diode in reverse bias with photon interaction.

Figure 9 - left, shows the inner configuration of the Photo-Diode. For some time the electrons of the n-zone will cross the pn-junction and diffuse into the p-zone, neutralizing the holes. A depletion-zone across the pn-junction will form. With electrons crossing from n-zone to p-zone, the p-zone will charge electrically negative and the n-zone electrically positive. The growing electric field will eventually stop the diffusion and an equilibrium will be build. Applying a battery to the Photo-Diode as shown in Figure 9 - right, the depletion-zone will grow. When a photon hits the depletion-zone, a photo-electron 'pe' (orange) will be generated that gets the energy of the photon as kinetic energy. The

'pe' will lift up from the valence-band into the conduction-band of the semiconductor or it will collide with electrons of the valence-band (red) and lifting them up into the conduction-band by exhausting its kinetic energy. The hereby generated free electrons (red) will cause a short electric current through the battery. With a resistor 'R' in the circuit, this current can be measured as a short voltage peak U_{t_0} every time a photon hits the diode. The actual way the photo-electric-effect takes place depends on the initial energy of the photons. Is their energy low, at a few electron-volts (optical light), the photo-electric-effect is running on electrons of the valence-band of the semiconductor only, when it has several kilo electron-volts (X-rays), it rather takes place on electrons of the k-shell of the silicon atoms.

4.3 The Charged-Coupled-Device (CCD)

The Charge-Coupled-Device (CCD) is a two dimensional array of Photo-Diodes that provides a light sensor with spatial resolution. Figure 10 shows a photograph of such a CCD sensor as it is used in modern astronomical cameras.
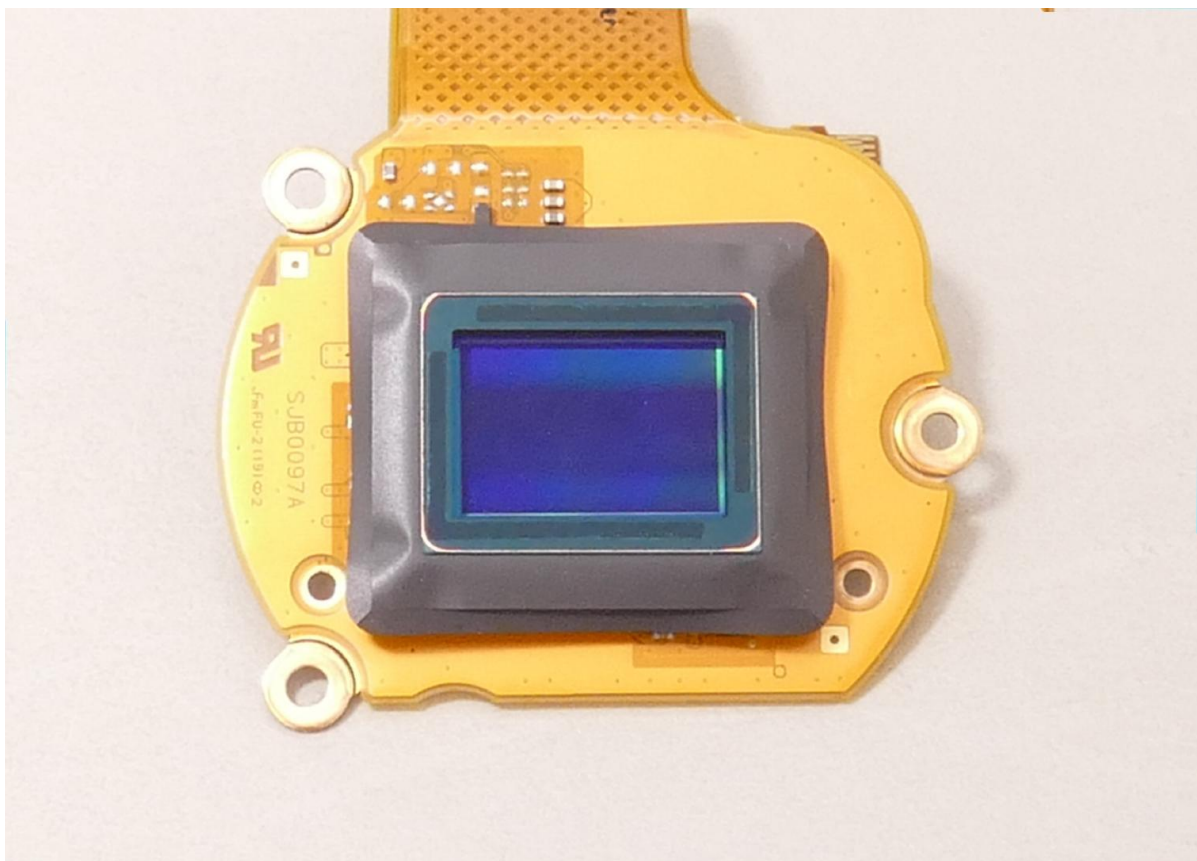

Figure 10: Photograph of a typical CCD-sensor. The 10 million pixels of the chip are much to small in order to see them in the photograph.

Figure 11 shows an illustration of six pixels of a larger CCD in cross section. The bulk of the CCD defines a pn-junction. When a voltage is applied between the n-layer and the p-layer in reverse bias, a depletion zone is growing at the pn-junction directly below the surface of the CCD, where photon interactions will be generating electron-hole-pairs by the photo electric effect. The generated holes will be drained through the negative p-contact of the chip but the generated electrons will stay confined inside the boundaries of the pixels when a positive voltage is applied to the center electrode of each pixel position.
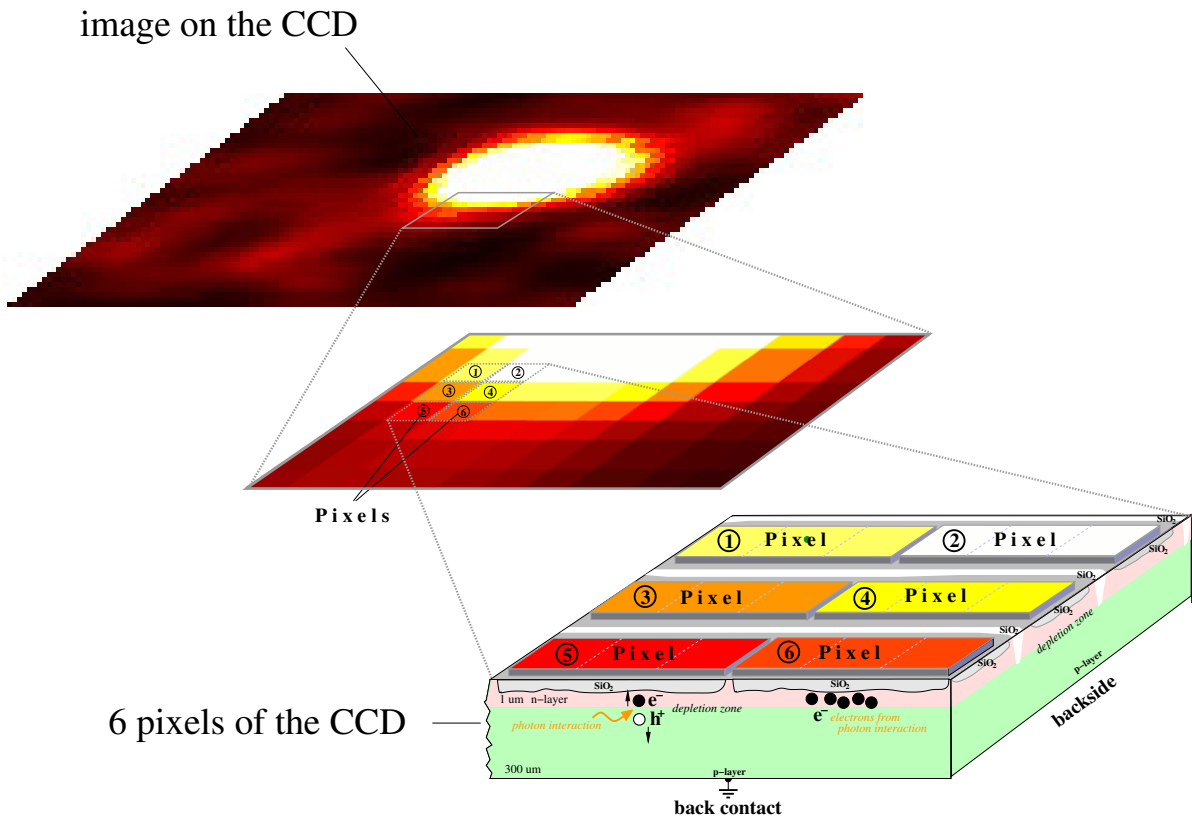
Figure 11: Cross section of a CCD sensor

A more detailed illustration of the CCDs setup is shown in Figure 12. Each pixel consists of three types of electrodes that define a pixel. The different types of electrodes are electrically connected to each other and can be connected to a positive electric voltage that creates a potential well below the center electrode (red) of each pixel. There are three Φ signals required in order to control the location and the movement of pixel-charges below the surface. The electric field of this Φ voltages confines the electrons generated by photon interactions inside the wells of the pixels. The electrodes are electrically isolated form the bulk of the CCD by a SiO_2 layer, SiO_2 is also used as channel-stops that isolates the rows of the CCD from each other, preventing dispersion of pixel-charges into the pixels of neighboring rows. There is no electric current going from the electrodes into the chip, the electrodes just control the charges inside the pixels by their electric

18

field.

For the readout of an image, all pixel-charges of the CCD must be moved through the bulk of the sensor towards the border, line by line, without loosing the pixel confinements. At the readout line, electronic amplifiers are attached that will sample the amount of charges contained inside of each individual pixel. Usually, all pixels of one line will be sampled simultaneously together. The readout chip must have as many channels as the CCD has pixels along a line. Finally, the sampled charges will be buffered inside the readout chip and serially readout through an Analog-to-Digital-Converter (ADC) for digitization. After a line is sampled and readout, the pixels of the readout line will be discharged and the image is moved one line further towards the readout line in order to readout the pixels of the next line. The procedure is succeeding until the whole image was readout completely.
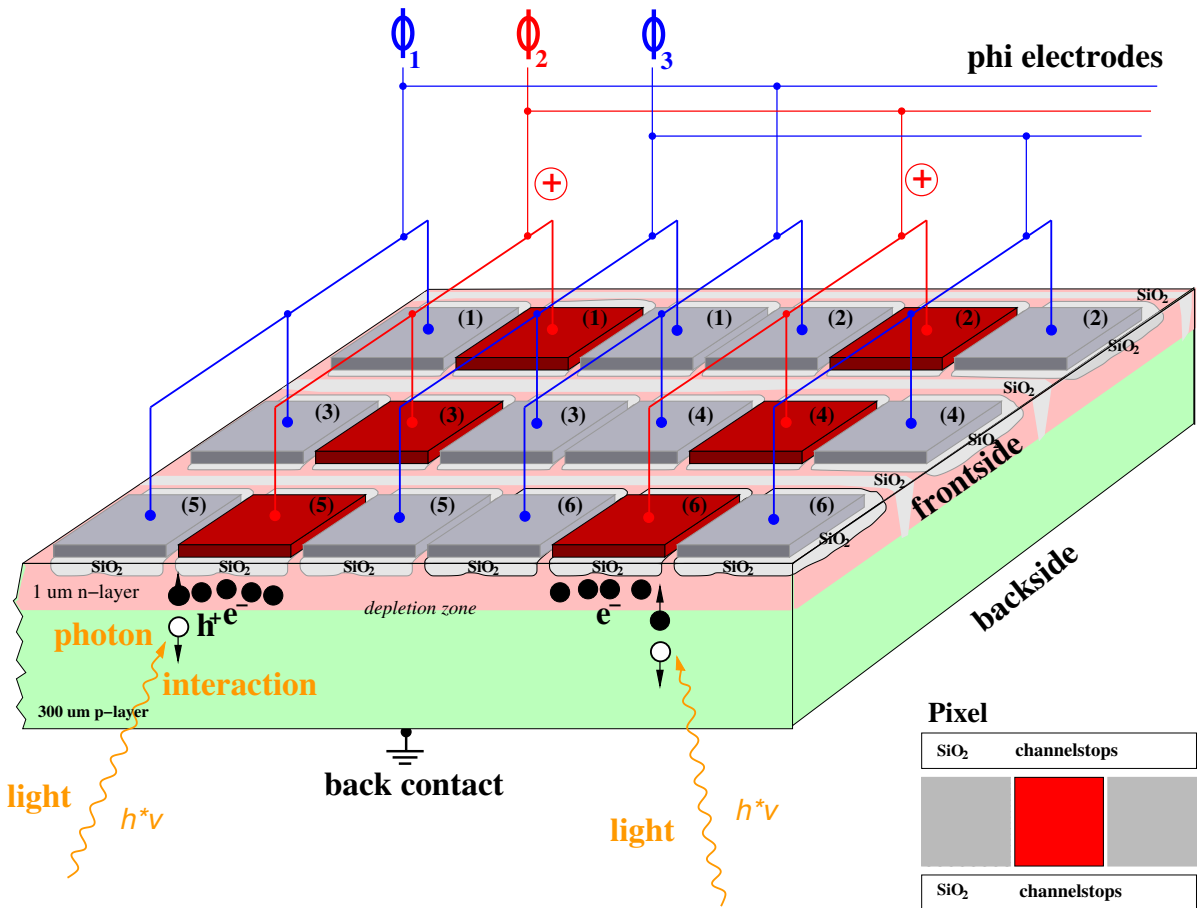

Figure 12: Cross section and electrical wireing of the CCD sensor

For the movement of charges towards the readout line, the voltages of the electrodes must be varied in a certain way. Figure 13 shows an illustration how the readout of an image can be controlled by the Φ-signals. The charges are moving from pixel position to

pixel position without loosing the confinement when the Φ signals are driven correctly. On the left side of Figure 13 is an illustration of such a sequence that transfers the image-charges by one line towards the right direction. The right side of Figure 13 shows the corresponding voltage modulation of the Φ-electrodes over time.

The operation of the CCD requires two distinct phases: a) **Exposure**, where the voltage settings of the Φ signals are constant, and b) **Readout**, where the voltage settings of the Φ signals will be varying over time. The illustration in Figure 13 shows the movement of charges by one pixel to the right, towards the readout line of the CCD. Considering a CCD with 1000 by 1000 pixels, 1000 of such successive sequences will be required in order to readout a complete image. The device that is generating and controlling the Φ signals during 'Exposure' and 'Readout' is called a **'Sequencer'** and often implemented as an ASIC[2] or as an FPGA[3] integrated electronic circuit. The electronics department of the IAAT has developed such devices for several cameras (XMM-Newton, eROSITA, ATHENA) in the past.

4.4 Astro Cameras

CCD cameras for astronomy applications usually have some different features compared to common consumer cameras. For one thing, astronomical cameras have no lenses or optical systems, since the telescope will provide this. Second, these cameras are optimized for low noise, since they must be working on very weak and dim sources. Therefore, most professional astronomical cameras provide a **cooling** system, usually in form of a Peltier-cooler (-20 °C), some very expensive systems are cooling their sensors by liquid nitrogen (-196 °C) or even by liquid helium (-270 °C). In all cases, astronomical cameras provide **'dark-imaging'** in order to reduce the background signals from thermal excitations, most systems also offer **'flat-field'** in order to remove hot and dead pixels. In order to support **'long-time-exposure'**, astronomical cameras often employ two separate CCD sensors. Besides the main CCD sensor for imaging, there is often a smaller CCD sensor that can be used for tracking objects and guiding the telescope onto the movement of faint light sources. Since CCD sensors can only record variations in brightness, not in color, astronomical cameras provide **'filter-wheels'** with a variety of color filters. In order to generate a color image, three exposures with 'red', 'green' and 'blue' filters are recorded and combined by computer software. The filters are also required for spectral classification of stars in the Hertzsprung-Russel diagram. Astronomical cameras usually have an improved **'Full-Well-Capacity'**, because they employ larger pixels compared to consumer cameras, meaning they can store a higher amount of charges per pixel which is gaining the signal to noise ratio of the image signals and improving the dynamic range of the sensor as well. Commercial astronomical cameras

---

[2]Application Specific Integrated Circuit
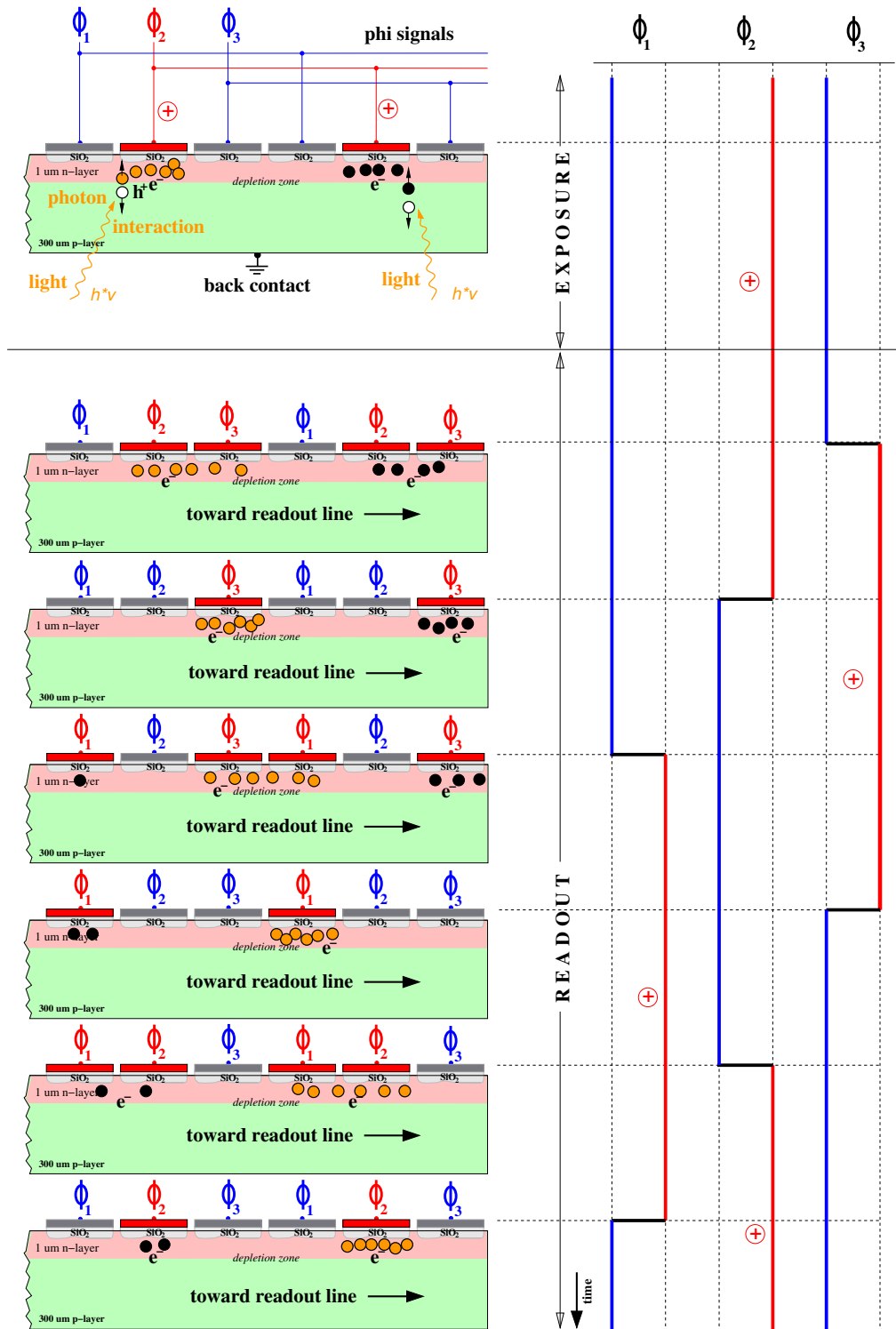[3]Field Programmable Gate Array

Figure 13: Readout of a CCD. The pixel-charges can be moved by voltage variations on the Φ electrodes without loosing confinement of the pixels. The illustration shows the movement of charges by one pixel. Notice, that each pixel consists of three Φ electrodes.

provide exposure times of up to 3600 seconds.

Figure 14 shows the anatomy of a commercial astronomical camera as it is used in the semi-professional field. The camera has a metal housing for heat dissipation. It employs two CCD chips, the main-CCD and a guiding-CCD for tracking purposes. There is a motor driven rotating shutter inside the camera housing that can close the aperture of the camera for automatic dark-imaging before every exposure. A motor driven filter wheel unit provides 5 possible filters for different applications. The camera is cooled by a Peltier system that is in direct contact to the main CCD sensor and can cool the sensor by 40 °C below the environmental temperature. A low vibration-fan is dissipating the heat from the back side of the camera. The camera is supplied with powerful software applications that provide a variety of image corrections, image processing and software based image stacking.
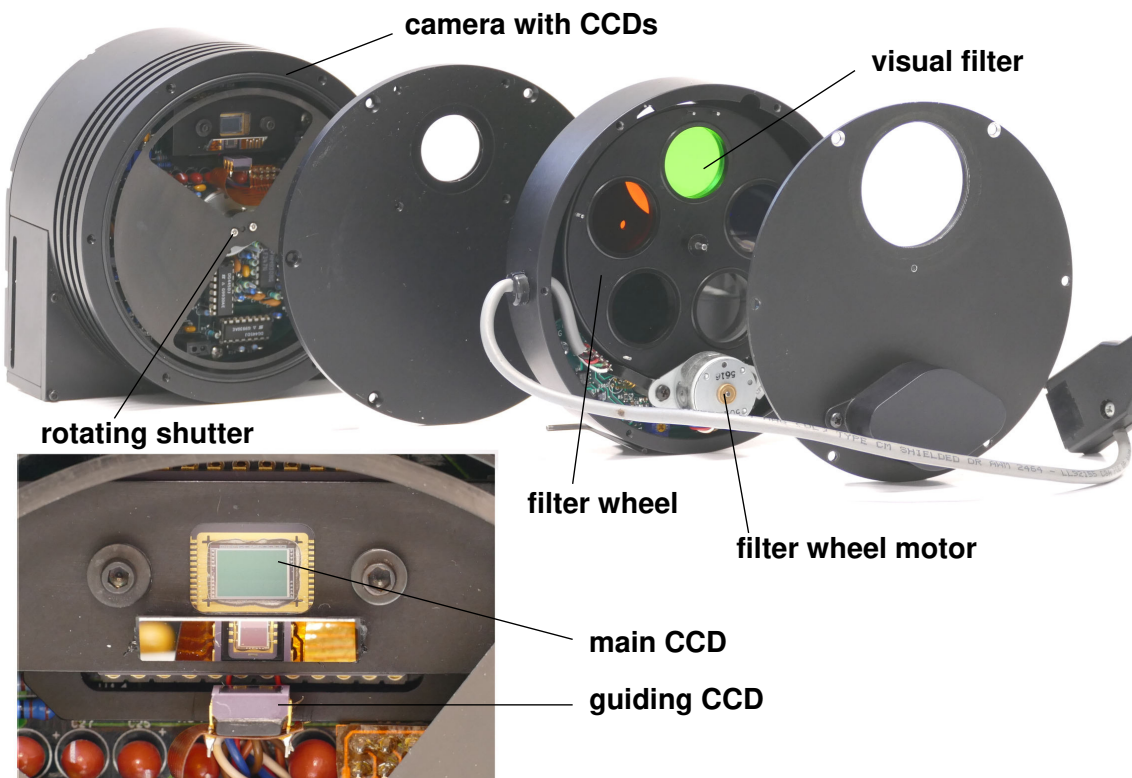
Figure 14: Anatomy of an astronomical camera. The camera is using two CCD chips, one for imaging and a second that can be used for guiding the telescope. A rotating shutter is used to generate dark-images for offset correction. A motor driven filter wheel can rotate different optical filters in front of the CCD for color imaging or for spectral classification of stars in the Hertzsprung-Russel diagram.

Figure 15 gives a block diagram of a typical CCD camera system. The camera has an analog part and a digital part. The analog part is containing the Charge Coupled De-

vice (CCD) light sensitive sensor that converts photons into electrical charges, an analog readout chip (ASIC[4]) that samples and amplifies the charge information into an electrical voltage and the analog to digital converter (ADC) that maps the electrical voltages to a range of binary numbers. The digital part is usually containing the digital signal processing (DSP) that is filtering and cleaning the image data from background signals, subtracting the dark current (offset correction), compensating for charge transfer loss (CTE) and so on. The pre processed data is send to a computer for further analysis, display and storage. In many cases, the computer is also incorporating the DSP functions in software and performing the data processing itself. A sequencer (SEQ) is generating all signals and timings that are required to drive the CCD sensor, the readout ASIC and the ADC. It also controls the function of the shutter, the filter wheel and the temperature cooler. In some sense, the SEQ is the heart of the camera while the DSP is its brain. The computer is commanding the camera but it can also guide the telescope by image informations if the camera employs also a guiding CCD.
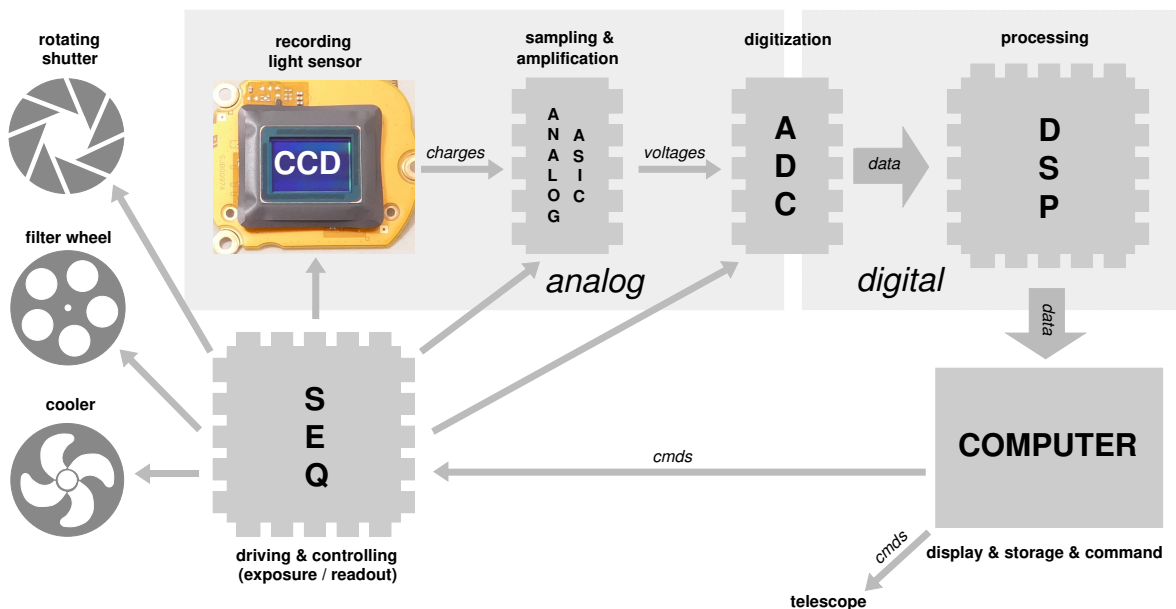
Figure 15: Block diagram of a typical camera system. The light is interacting inside the sensor, generating charges. The charges are sampled into voltages and amplified during readout by an ASIC, converted into digital data by an ADC and corrected by digital signal processing. Finally a computer will receive the recorded image for display and storage.

The IAAT currently operates two cameras at the 80 cm telescope:

- SBIG-STL1001E astronomical camera employing a CCD chip with 1024 by 1024 pixels, auto-dark, Peltier cooler, 5 position filter wheel and an 16 bit ADC.

---

[4]Application Specific Integrated Circuit

- ZWO-ASI294 MOS Camera, employing a color MOS sensor with 4144 by 2822 pixels, Peltier cooling, video capability and an 14 bit ADC.

5 Spectrographs

A spectrograph is an instrument that is dispersing light into its spectral contributions, named a spectrum. The spectrum displays the intensity of light as a function of the wavelength. It can reveal a multitude of information about the source, the elements contained, the physical processes involved, its temperatures, velocities, the strength of gravitational and magnetic fields present at the source but also the occurrence and composition of the interstellar medium between the source and its observers on Earth. The spectrum provides a unique kind of signature for each individual light source.

The general schematics of a spectrograph are shown in Figure 16. Central elements of the spectrograph are the slit 'S', the collimator 'C' and the dispersing element 'G'. Light, that is entering from the telescope is passing the slit and will be converted into a plane and parallel wavefront by the collimator before it falls on the dispersing element. The dispersing element is either a prism or an optical grating, the grating is often preferred because of its better linearity and resolving power. By the dispersing element, the light is dissolved into its spectral constituent parts. Behind the dispersing element, a lens 'L' is focusing the spectrum onto the plane of a CCD detector where an image of the spectrum can be recorded.
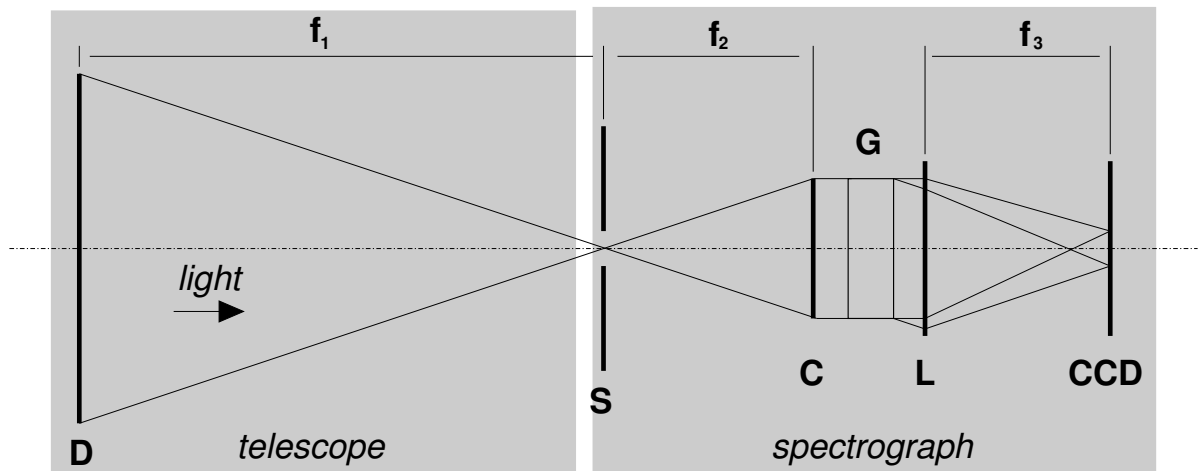
Figure 16: The spectrograph will be directly attached to the 80 cm telescope. The main mirror 'D' of the telescope has a focal length 'f_1' of 6.4 meters and is reflecting the light directly onto the slit 'S' of the spectrograph. A collimator 'C' directs the light onto the grating 'G' for dispersion and a CCD camera is recording the spectral image of the astronomical object that is adjusted to the slit of the spectrograph.

The slit of the spectrograph is used to select an object in the field of view of the tele-

scope that is scheduled for spectroscopy. Even with the accurate guiding of the telescope mount it can be difficult to keep the selected object onto the slit of the spectrograph all the time during a long time exposure. Therefore, some spectrographs also provide an additional sensor that is tracking the selected object above the slit and controlling the telescope slewing during spectroscopy. For grating spectrometers, two different gratings are common, a):transmission gratings and b):reflection gratings, the 10C spectrograph of the IAAT is using a reflection grating.

5.1 The grating

Reflection gratings employ a large number of grooves that are carved onto a glass body by a diamond needle. Modern spectrographs have numbers between 10000 and 1 Million grooves per grating and count for the crown achievements of precision mechanics. The grooves are blocking the light, while the glass in between is reflecting. Reflection gratings are preferred to transmission gratings, since they do not suffer from transmission loss and provide brighter spectral imaging. The theory for transmission-gratings and for reflection-gratings is the same and illustrated in Figure 17.

When a coherent wavefront of light enters the grating, the transmitted or reflected parts will be interfering constructively for those diffraction angles where the path difference between two consecutive light paths is an integral number 'k' of the wave length. The integral number 'k' defines the spectral order of the diffraction. Higher orders have a better lateral spectral resolution but provide a dimmer signal. A common problem is, that different orders can superpose each other making it difficult to identify which part of the spectrum belongs to a particular order. A further problem, while the spectra of higher orders have large lateral deflection angles, this requires a very long and narrow sized detection sensor. Unfortunately, such long shaped CCD detectors are very hard to produce and come by, why a new class of spectrometer type have been invented, the 'Echelle' spectrometer. The Echelle-spectrometer folds the higher orders of the diffraction into a two dimensional plane and such a spectrum can be photographed easily by a common rectangular shaped CCD sensor.

From Figure 17 we find Equation 5 for the maxima of the diffraction:

$$sin(\beta) = \frac{k\lambda}{g} \tag{5}$$

where 'k' is an integer number, the order of diffraction, and 'g' is the grid constant in units of 'meter'. Since white light contains colors of different wavelength λ, the different colors will produce maxima at different angles 'β' and dispersing into a multitude of angles creating a spectrum. Shorter wavelength (blue light) will be deflected less, longer
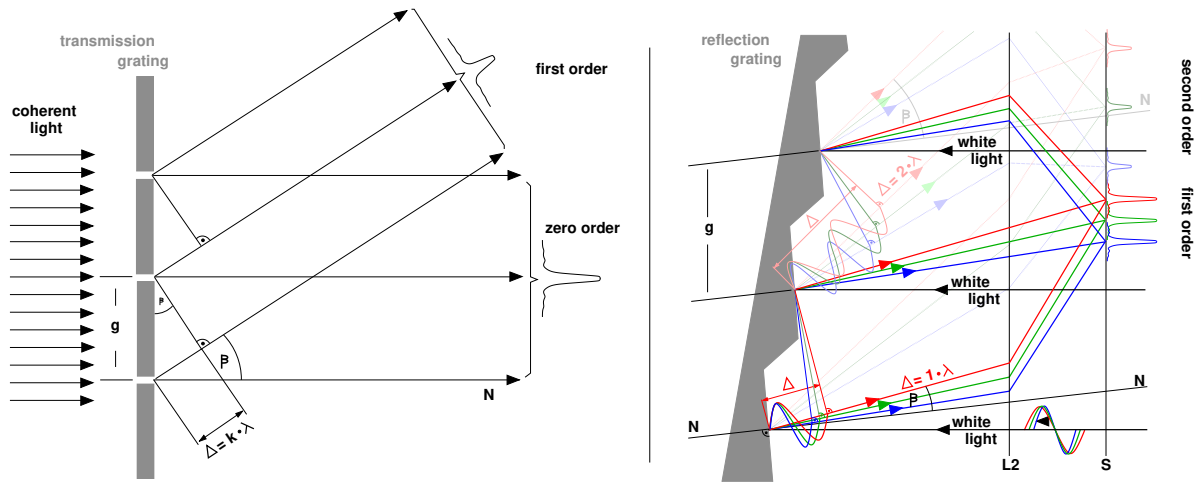
Figure 17: The light path for transmission grating (left) and for reflection grating (right). The maxima of interference are at path length differences $\Delta = k * \lambda$, where 'k' is the order of the spectrum. Higher orders of k produce usually better spectral resolutions, but also dimmer spectral images.

wavelength (red light) will be deflected more.

The spectral resolution of the spectrograph is defined, where the intensity distribution for two lines of the wavelength λ and $\lambda + \Delta\lambda$ can be barely recognized as separate. This is the case when the main maxima of one line falls together with the first minimum of the adjacent line. The ratio in Equation 6 is called the spectral resolution of the spectrograph:

$$R = \frac{\lambda}{\Delta\lambda} \tag{6}$$

where 'R' is the spectral resolution, λ the wavelength of a spectral line and $\Delta\lambda$ the smallest difference in wavelength to an adjacent spectral line. For a grating spectrograph, this ratio is defined by Equation 7:

$$\frac{\lambda}{\Delta\lambda} = Kk \tag{7}$$

where 'K' is the number of carves of the grating that are illuminated and 'k' the spectral order. In theory, the spectral resolution of the spectrograph only depends on the number of carves of the grating and on the spectral order that will be observed. For real implementations however, the spectral order depends also on the precision of the grating and on the width of the entrance slit of the spectrograph.

5.2 The 10C Spectrograph

Figure 18 shows a photograph of the 10C spectrograph as it is employed by the IAAT. The 10C spectrograph contains a reflection grating as dispersing element, its internal setup is illustrated in Figure 19. The light of the telescope is entering from above and will be passing the 'slit (S)' on its way to the 'collimator (C)' where it is converted into a parallel wave front and reflected back onto the 'grating (G)'. The grating is dispersing the light into a spectrum that is focused by a 'lens (L)' onto a CCD camera.
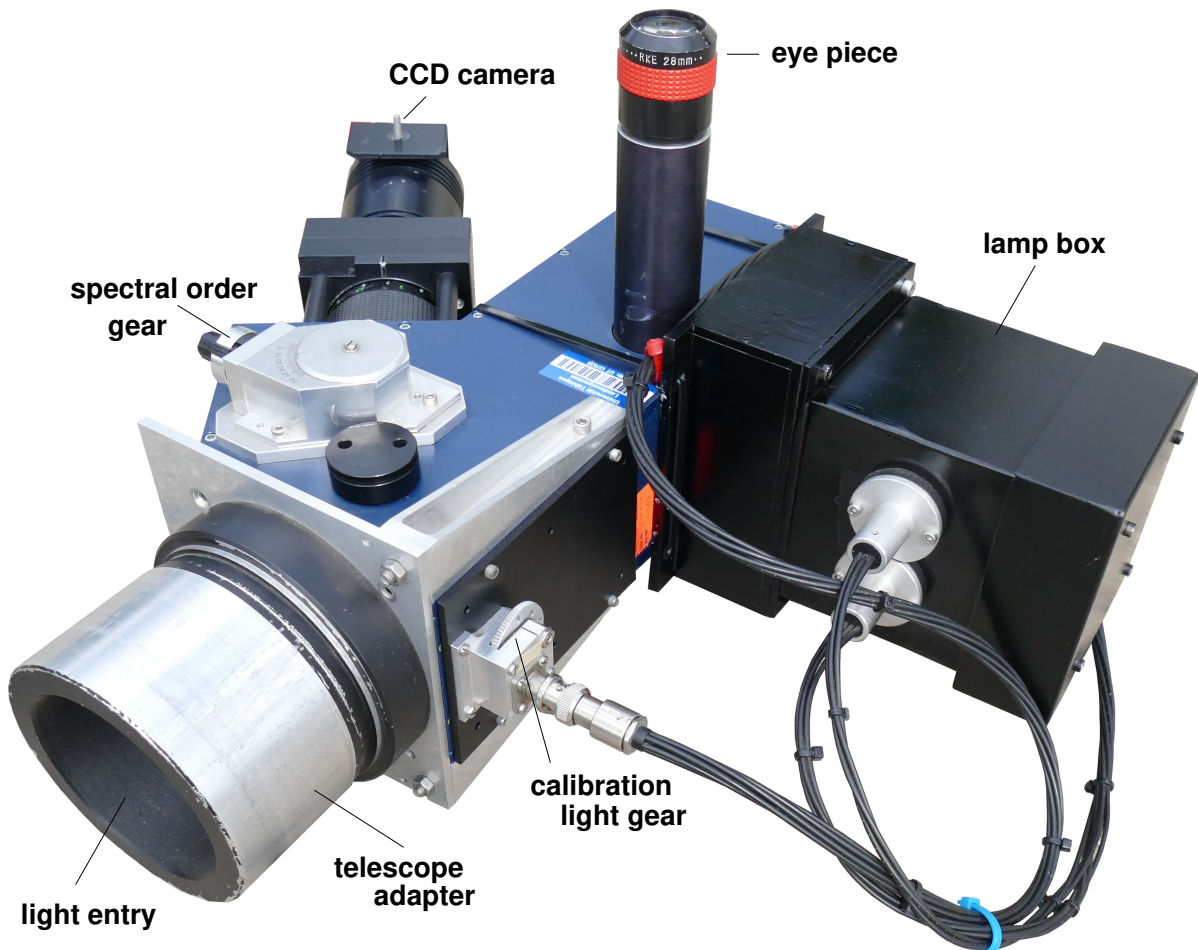
Figure 18: The 10C spectrograph of the observatory, it will be mounted by the 'telescope adapter' onto the Nasmyth focus of the 80 cm telescope. An object can be adjusted onto the slit of the spectrograph when looking through the 'eye piece'. The dispersed light will be photographed by a 'CCD camera'. Since the field of view of the camera can not cover the complete spectrum at once, the spectral range must be selected via the 'spectral order gear'. Attached to the spectrograph is a 'lamp box' that contains a Neon and a Mercury light source for optional wavelength calibration. The calibration light is led by fiber optics onto the slit of the spectrograph and can be photographed together with the spectrum of the object of investigation.
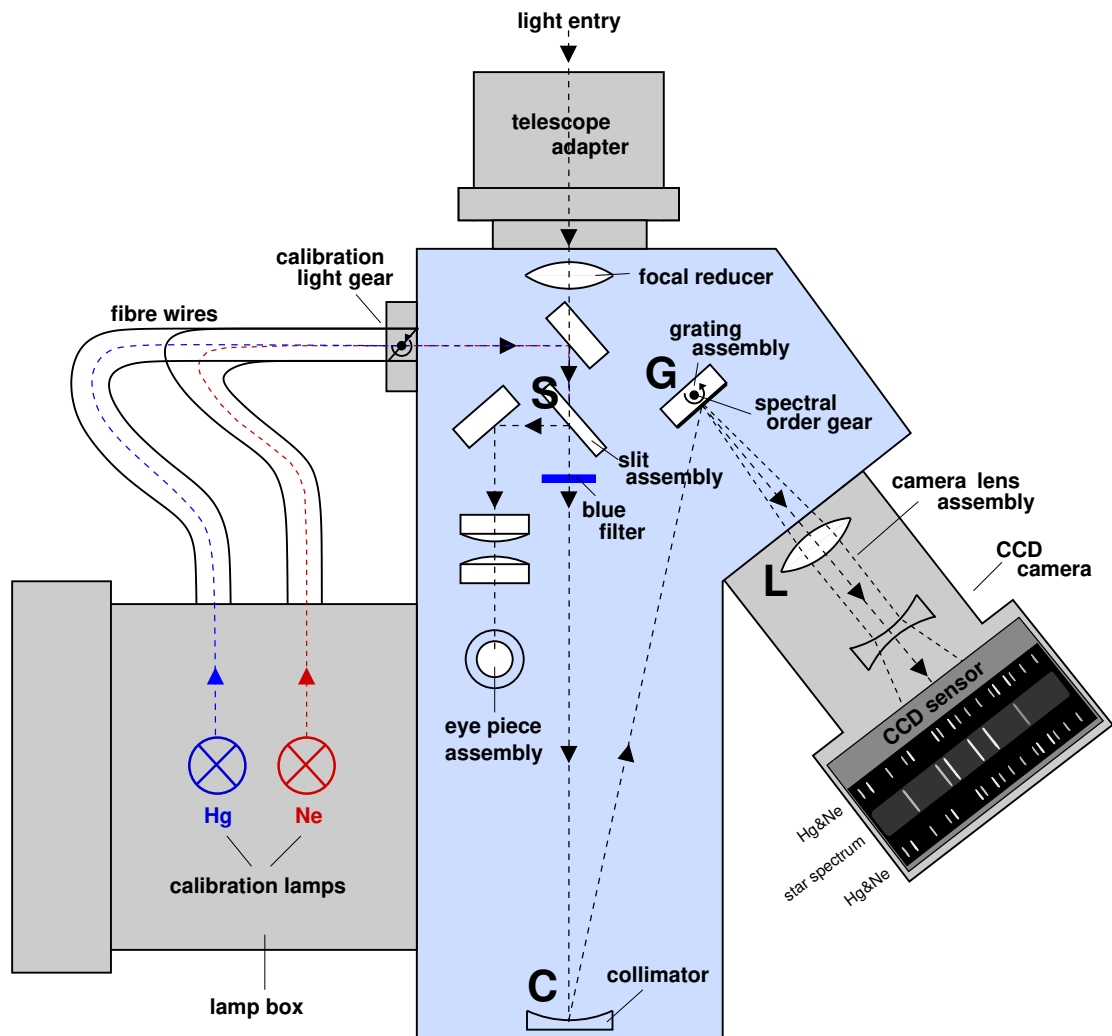
Figure 19: Drawing of the internal setup of the 10C spectrograph of the IAAT. The spectrograph will be attached to the 'left focus' of the telescope. The object that is scheduled for spectroscopy will be manually adjusted onto the main slit by using the eye-piece of the spectrograph. A CCD camera is recording the spectral image of first order of the source, together with the spectral image of the Neon- and the Mercury calibration lamps. A spectral-FITS-image is generated on the 'Spectroscopy Computer' of the observatory that must be transferred onto the lab course laptop computers for further data analysis.

The actual implementation of such a spectrograph has some additional features. The slit assembly contains additional slits for calibration sources that are required to calibrate the recorded spectra onto actual wavelength numbers. As calibration sources, a lamp assembly is attached to the spectrograph that contains a Neon lamb and a Mercury lamp. Both lamps provide certain emission lines in their spectra that are tabulated and exactly known by their wavelengths. The slit assembly will display the calibration lines together with the main spectrum of the source onto the field of view of the CCD camera. Comparing the position of spectral features of the source to the emission lines of the Neon- and Mercury lamps allows the calibration of the spectrum into wavelengths.
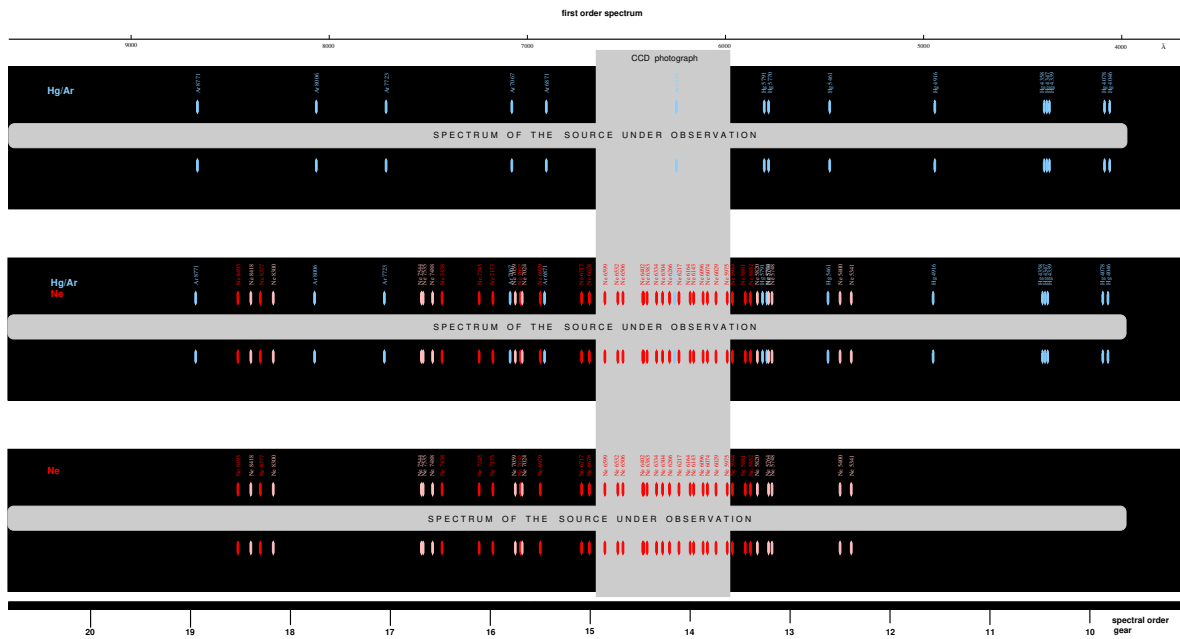
Figure 20: Full first order spectral image of the calibration lamps recorded by the 10C spectrograph. The shown spectral image is assembled from 10 spectral- FITS-images that were photographed at different 'spectral order gear' settings between 10 and 20 into a full optical spectral image between 4000 Å and 8000 Å. On the top is the spectral image of the Argon/Mercury lamp alone, on the bottom the spectral image of the Neon lamp alone. In between is the spectral image of both calibration lamps together. All spectral emission line have been identified from tabulated spectra. The spectral image here contains no source, it was taken from the calibration lamps alone. The gray column marks the field of view of the CCD camera at a 'spectral order gear' setting of 14.

Figure 20 shows the spectral image first order of the calibration lamps. On top there is the spectral image of the Argon/Mercury lamp alone, on the bottom the spectral image of the Neon lamp alone. In the middle, there is the spectral image of both lamps together. In the white bar between the spectral lines usually the spectral image of the source that is adjusted on the main slit is displayed. All spectral lines are marked by

29

their wavelength, the range goes from 4046 Å on the blue end of the spectrum to 8771 Å on the red end.

Attached to the slit-assembly is the eye-piece assembly of the spectrograph. The eye-piece is used to adjust the object that is scheduled for spectroscopy onto the main slit of the slit-assembly by manually slewing the telescope. There is also a blue-filter available that can be put into the optical path of the spectrograph. The blue-filter is opaque at wavelength below 5100 Å. It is used at wavelength above 7500 Å to avoid the contamination of first order spectral lines by spectral lines of the second order.

The grating can be rotated by the 'spectral order gear' of the spectrograph. This allows to bring different parts of the spectrum into the field of view of the CCD-Camera. The field of view of the CCD usually covers only a fraction of the spectrum, the spectral images in Figure 20 were assembled from 10 distinctive photographs. In most cases, only the first order spectrum is used. The first order spectrum can be recorded when the spectral order gear is set to a range between settings 10 to 20. The second order is between setting 21 and 33. Higher order spectra usually have a better spectral resolution but suffer from lower signal to noise ratio. The intensity of the calibration lamps in relation to the intensity of the main spectrum can be adjusted by the 'calibration light gear' of the spectrograph.
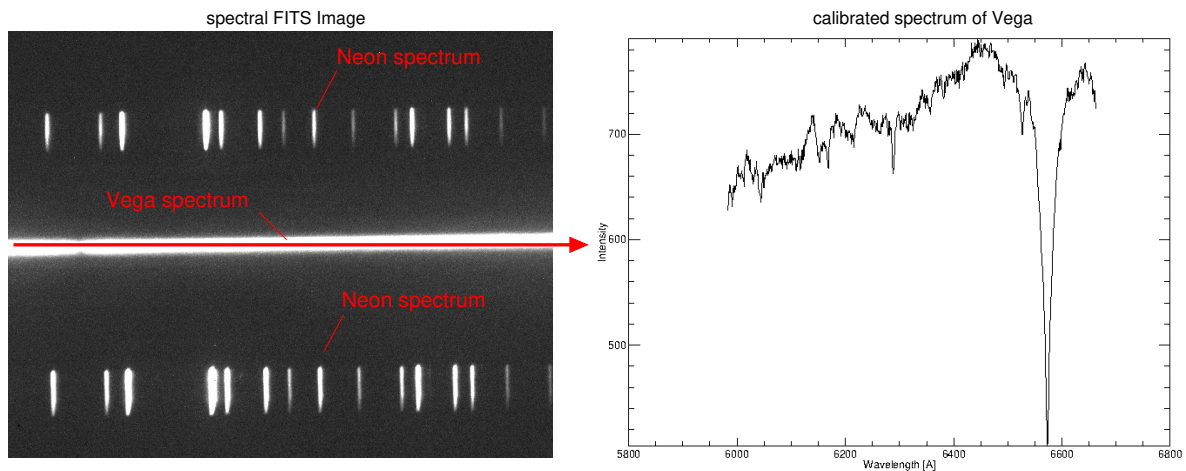
Figure 21: Example for a star spectrum, taken from the star 'Vega'. For the lab course, usually only a single spectral image (left) is taken at an interesting part of the full spectrum, compare the gray shaded part in Figure 20. The example contains the spectral image of the Neon-calibration source together with the light of 'Vega' in between. The spectral image of 'Vega' is too bright in order to recognize any details without spectral analysis. After the IDL/GDL data analysis however, the spectrum (right) can be plotted and reveals the full features of the 'Vega' star spectrum.

The CCD-Camera of the spectrograph will be connected via an USB 1.1 interface to

the 'Spectroscopy Computer' of the observatory. The computer runs the 'Maxim-DL' software for recording spectral images. All images will be stored in FITS file format and can be analyzed by the IDL/GDL scripts that are provided by the lab course laptop computers. Figure 21 shows an example of such a recorded spectral-FITS-image generated from the star 'Vega'. On the left side is the spectral image. It shows a range between 6599 Å (most left Neon line) and 5975 Å (most right Neon line) and corresponds to a cut out of the spectrum shown in Figure 20 at a spectral order gear setting of 14. On the right side are the IDL/GDL analyzed spectra for the observation source Vega (above) and the Neon calibration source (below). The calibration generates a range on the x-axis for wavelength between 5800 Å and 6800 Å.

The IAAT currently operates two spectrographs at the 80 cm telescope:

- 10C slit spectrograph using a reflection grating and a Starlight HX9 CCD camera, 600 carves per mm, maximum first order at 5000 Å, spectral resolution $\lambda/\Delta\lambda = 840$ @ 5000 Å.

- BACHES Echelle spectrograph using an SBIG STF 1603 CCD camera, spectral resolution $\lambda/\Delta\lambda = 10000$ @ 5000 Å.

6 Photometry

Photometry is a standard technique in astronomy that is recording the brightness, color and light curves of celestial objects. Utilizing the Hertzsprung-Russel diagram, it can be used to determine the distance and the age of star clusters as it will be demonstrated in this lab course.

6.1 The radiation of a star

The spectral radiance of a black body in thermal equilibrium is defined by the Planck law, shown in Equation 8 and illustrated in Figure 22:

$$B_\nu(T) = \frac{2h\nu^3}{c^2} \frac{1}{e^{h\nu/k_B T} - 1} \tag{8}$$

where 'B_ν' is the spectral radiance, 'h' the Planck constant $h = 6.626 * 10^{-34} Js$, 'ν' the frequency of the radiation, 'c' the speed of light, 'T' the temperature of the black body and 'k_B' the Boltzmann constant $k_B = 1.380 * 10^{-23} J/K$. Therefore, the total emitted radiation flux 'F^+' of an object can be calculated in Equation 9 as:

$$F^+ = \pi B(T) \tag{9}$$

considering the Stefan-Boltzmann law, this is also proportional to the 4th power of the temperature of the object, leading to Equation 10:

$$F^+ = \pi B(T) = \sigma T^4 \tag{10}$$

where 'F^+' is the total radiated flux, 'σ' the Stefan Boltzmann constant $\sigma = 5.67 * 10^{-8} W m^{-2} K^{-4}$ and 'T' the temperature of the body. Therefore, the total radiation of a black body is proportional to the 4th power of its temperature.

Although stars are not in a thermodynamic equilibrium and their energy distribution is not that of a black body, the Planck law can still be used in approximation. Comparing the total radiated flux of a star to that of a black body, we can define the effective temperature 'T_{eff}' of a star, given by Equation 11:

$$\sigma T^4 = \pi B(T) = F = \sigma T_{eff}^4 \tag{11}$$

Therefore, the effective temperature 'T_{eff}' of a star is those temperature of a black body 'T' that would radiate the same amount of energy per unit area and unit time. This can
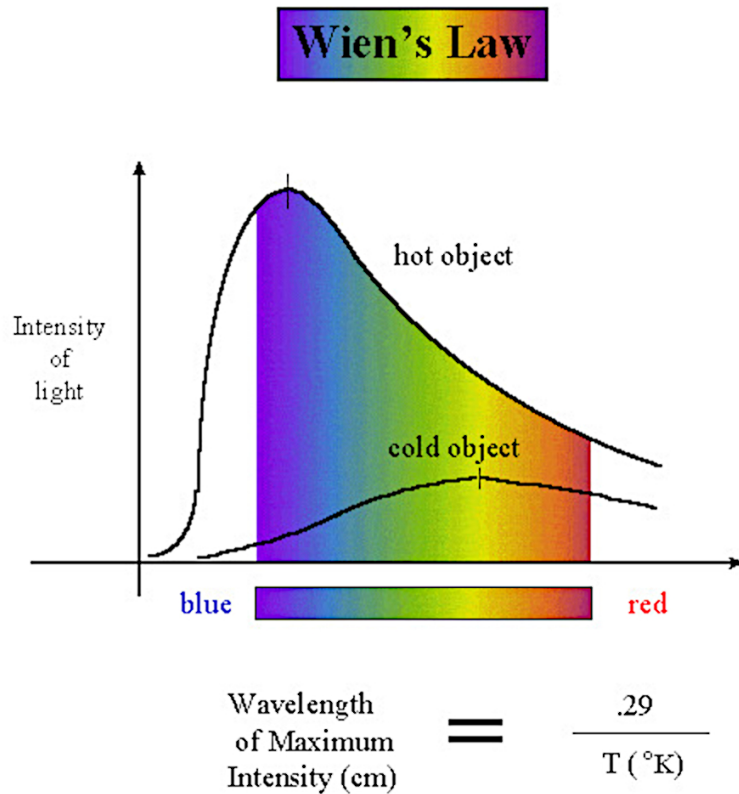
Figure 22: Planck law and Wien's law of displacement. The maximum of radiation is inverse proportional to the temperature of the black body. The hotter the black body, the more is the maximum of intensity shifted towards shorter wavelength (blue end) of the spectrum.

be used to define the 'luminosity' 'L' of a star. It is the total amount of energy radiated per time and can be calculated as the product between the total radiated power 'F' and the surface area of the star as shown in Equation 12:

$$L = 4\pi R^2 F = 4\pi R^2 \sigma T_{eff}^4 \tag{12}$$

Therefore, the luminosity 'L' of a star is only a function of its surface temperature 'T' and its surface area '$4\pi R^2$', where 'R' is the radius of the star.

6.2 The magnitudes of the stars

The **apparent magnitude 'm'** is the magnitude that a star is appearing to an observer on Earth. Its definition goes back to the antique. The greek originally had define 6 magnitudes to describe the brightness of the stars, where the brightest stars had a

magnitude 'm=1' and the dimmest stars a magnitude 'm=6', while the difference of brightness between m=1 and m=6 has a factor of 100 and the difference between two adjacent magnitudes 'm_n' and 'm_{n+1}' is a factor of 2.512.

Later on, the definition of the apparent magnitude 'm' was defined in a logarithmic scale shown by Equation 13 that is matching the historic definition as well as extending it to dimmer and brighter sources:

$$m_1 - m_2 := -2.5 \; log(I_1/I_2) \tag{13}$$

In this law, 'm_1', 'm_2' are the magnitudes of two different stars and 'I_1', 'I_2' the corresponding intensities. Notice, that the law can not be derived from somewhere, its a definition. The factor of 2.5 was chosen to match the classical classification.

Equation 13 describes the apparent magnitude 'm' as the difference between two objects and connects it to the flux of the light sources that can be measured on Earth. In order to give an absolute value for the apparent magnitude, a reference is needed. Initially the star 'Vega' (αLyr) was defined as such a reference and was defined to have an apparent magnitude of 'm=0 mag'. Meanwhile, these reference has been extended to a whole catalog of 96 stars, where Vega is only one of them and has an apparent magnitude of m=0.03 mag. Some other examples for apparent magnitudes are the Sun m=-26.8 mag, Sirius m=-1.6 mag or Polaris m=1.97 mag.

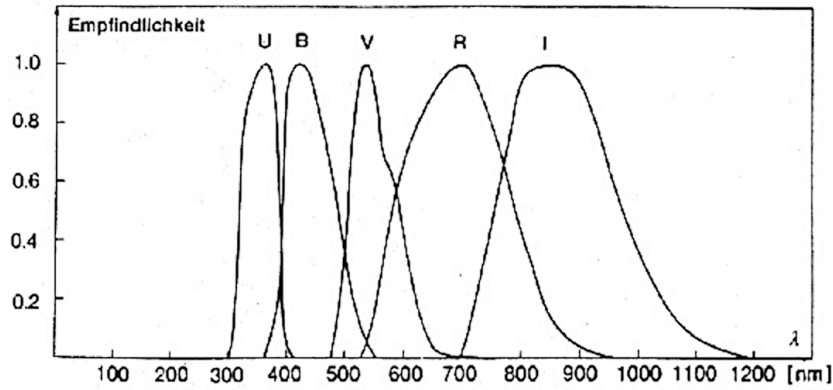**Figure 23:** Filter function of the Johnson system (U, B, V, R, I) (Credit: Unsöld & Bachek, 1988)

Today, the brightness is measured by CCD sensors that are making use of color filters. Magnitudes at different filter colors are labeled by an index. A common filter system was introduced by Johnson and Morgan, its filters are shown in Figure 23, the corresponding wavelengths of maximum transmission are listed in Table 1.

Table 1: The color filters of the Johnson system.

Symbol	Color	Wavelength λ_{eff}[Å]
U	ultra violet	3500
B	blue	4350
V	visuell	5550
R	red	7100
I	infrared	9700

The difference in magnitude of a star for different filters is called **'color'**, where always $m_{short-wavelength} - m_{long-wavelength}$ is given. This is true because the spectrum of stars follows nearly a black body and the measurement of only two different points in the spectrum can already determine the color of the star and therefore its temperature and spectral class. Because of the relative definition of the apparent magnitude, the zero point can be freely chosen. It is commonly calibrated to the star 'Vega', that should have a value of 0 in all filters.

6.3 The absolute magnitudes of the stars

In order to find a measure for brightness that is independent from distance, the **absolute magnitude 'M'** was defined as the apparent magnitude an observer would measure at an equal distance of 10 parsec (10 pc) to any objects. In this measure, the sun has an absolute magnitude of 4.8 M, that is the apparent magnitude the sun would appear at a distance of 10 pc from Earth. The difference between absolute magnitude 'M' and apparent magnitude 'm', **(m - M)** is called the **Distance-Modulus** because its only depending on the distance 'r' between the object to the observer, the formula is shown in Equations 14 and 15:

$$(m - M) = 5 \ log(r) - 5 \tag{14}$$

$$M = 5 - 5 \ log(r) + m \tag{15}$$

Assuming a distance of r = 10 pc and expressing the distance 'r' as 'r = r*/pc', Equation 15 would be evolving into:

$$M = 5 - 5 \ log(10pc) + m = m \tag{16}$$

and therefore, Equation 16 is exactly reproducing the definition: M = m @ r = 10 pc.

In reality, interstellar extinctions must also be considered. Extinction is the absorption and scattering of electromagnetic waves by dust and gas between an astronomical source and the observer on Earth. It can be added to Equation 14 as an additional term A_ν, transforming it into Equation 17:

$$(m - M) = 5\ log(r) - 5 - A_\nu \tag{17}$$

6.4 The Hertzsprung-Russel diagram

In the Hertzsprung-Russel (HRD) diagram, the stars are plotted by their absolute magnitudes 'M' against their surface temperatures or against the spectral classification. Figure 24 is showing the HRD of the neighboring stars of our sun. Small brown dwarf stars will populate the lower right of the diagram, having spectral classes 'K', 'M' or 'L', absolute magnitudes between 10 Mag to 15 Mag and surface temperatures of 1000 to 3000 Kelvin, while large blue giant stars are at the upper left, at spectral classes 'O', 'B' or 'A', absolute magnitudes of -10 Mag to 0 Mag and surface temperatures of 10000 to 50000 Kelvin. Our sun, as a small yellow star, is somewhere in between at spectral class 'G', an absolute magnitude of 4.8 Mag and a surface temperature of about 6000 Kelvin. The stars occupy the main branch of the HRD the longest time of their lifes, but leaving it when their nuclear fuel is exhausted. The evolution of stars can be traced throughout the HRD. The main branch is also called the **'main sequence'**. This is because when stars are forming from a gaseous cloud and start shining, they appear on the 'main sequence', where they stay the most time of their lifetime.

From calculated star models, the surface size, temperature and spectral class of a star can be estimated. The models also predict the lifetime for stars of a particular spectral class, since the lifetime is depending on the reserves of nuclear fuel and on the amount the fuel is consumed by nuclear fusion. The larger and hotter the star, the shorter the lifetime. Brown dwarf stars have an estimated lifetime of about 20 billion years or longer, while blue super giant stars only last for some million years.

6.5 The Color-magnitude diagram

The Color-Magnitude-Diagram (CMD) is for the apparent magnitude 'm' what the HRD is for the absolute magnitude 'M'. The CMD is one of the foundations of stellar astrophysics. The color is a measure for the effective temperature of an observed star and its apparent magnitude 'm' is a measure for its luminosity. When observing a cluster of stars from Earth, the extend of the cluster will be much smaller than its distance, all stars will have approximately the same distance from Earth. Therefore, the differences in magnitude of the stars of the 'main sequence' will be directly reflecting their differences in luminosity.
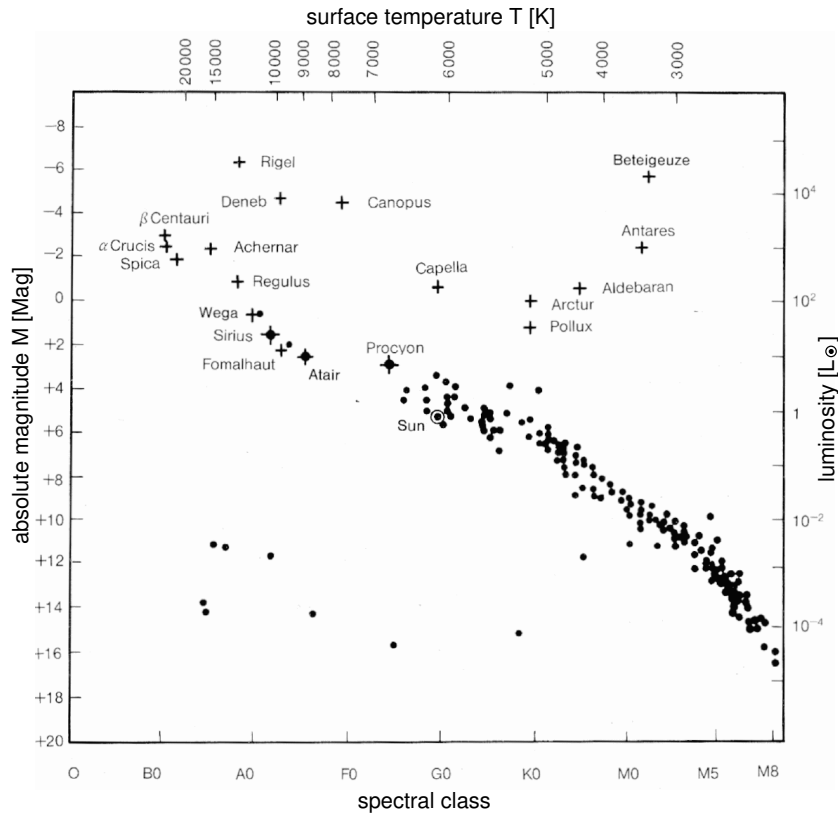
Figure 24: Hertzsprung-Russel diagram of night sky stars, (Credit: Karttunen & Kröger et al., 1987)

When recording the CMD of a star cluster as shown in Figure 25, the CMD is reproducing the HRD. Instead of spectral classes or temperatures, the x-axis of the CMD will be labeled just by color values (B-V) while the y-axis is labeled by apparent magnitudes 'm' (V) instead of absolute magnitudes as for the HRD. As we have already seen in Chapter 6.3, we can determine the color of a particular star just by measuring its intensity with a CCD sensor in two different colors, with the 'blue' and the 'visual' filter. This will give us the x-axis position of the particular star, while the brightness that the CCD sensor is recording will give us the magnitude position on the y-axis. For a cluster of dozens or hundreds of stars, we will record a CMD that looks pretty much like the HRD, since the star cluster will contain most probably stars of different sizes (magnitudes) and different spectral classes (colors). Figure 25 is showing a typical CMD of a star cluster, comparing it to the HRD Figure 24, we can identify in both the 'main sequence'.

In the photometry experiment of this course we will photograph a star cluster and manufacture a CMD from the taken blue and green pictures. The CMD will contain a 'main sequence' of stars that are in their prime years and hopefully a few very bright stars at the upper part of the CMD that have already exceeded their nuclear fuel and reached the end of their lifetime. These dying 'end of lifetime'- turn-off stars will leave the main
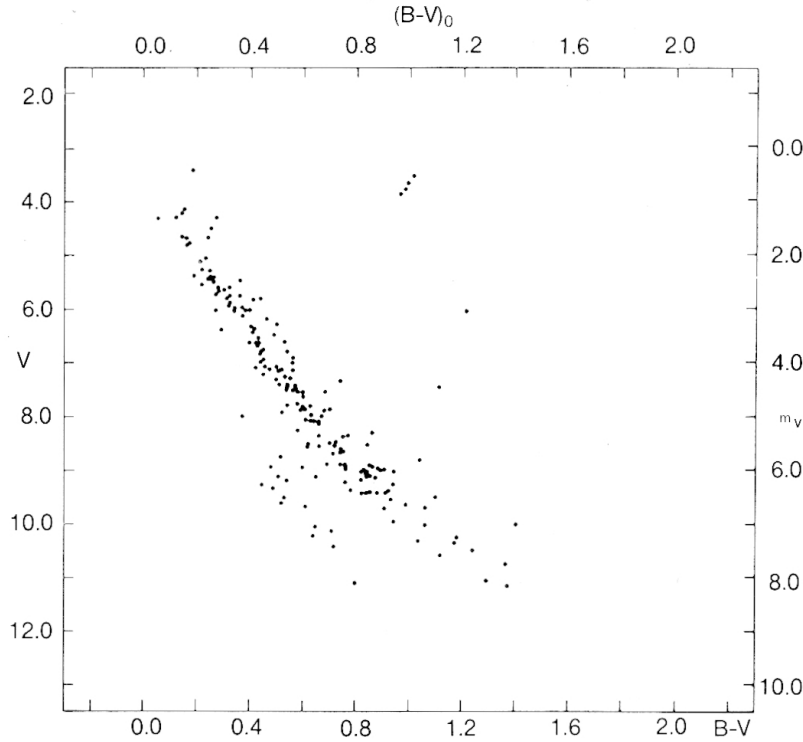
Figure 25: Color-Magnitude diagram of the Hyades star cluster, (Credit: Karttunen & Kröger et al., 1987). 'V' is the apparent magnitude in the 'Visual' filter (green) and 'B-V' the color of the stars, which is the difference of magnitude between the 'Blue' filter and the 'Green' filter.

sequence and turn-off to the right into the region of red giant stars of the CMD. Since the CMD is not calibrated, we can not directly determine the total magnitudes 'M' of the stars, we only know the apparent magnitudes 'm' so far. But we can overlay the CMD to the HRD and shift the 'main sequence' of the CMD along the y-axis until it matches the 'main sequence' of the HRD. From this shift, we can learn two things: (1) the distance of the star cluster from Earth and (2) the age of the star cluster.

6.5.1 The distance of star clusters

By shifting the 'main sequence' of the CMD onto the 'main sequence' of the HRD, we determine (m - M), the Distance-Modulus. Is the shift zero, the Distance-Modulus is also zero and the distance to the star cluster is 10 pc according to the definition in Equation 14. For all other shifts, we can determine the distance of the star cluster 'r' from Earth when we are determine the Distance-Modulus of the shift and resolving Equation 15 into Equation 18:

$$r = 10^{\left[\frac{1}{5}(m-M) + 1\right]} \tag{18}$$

6.5.2 The age of star clusters

The lifetime of the stars that are plotted on the main sequence of the HRD can be calculated from star models. The heavier a star is, the sooner it is exhausting its fuel and leaving or 'turning-off' from the main sequence. Using the 'Turn-Off' method, we can determine the age of an open star cluster. For this, we will shifting the main sequence of the CMD onto the main sequence of the HRD and then looking for the turn-off point, where stars are leaving the main sequence of the CMD. This turn-off point will start at the highest magnitudes for young star clusters and move down to lower magnitudes, the older a star clusters becomes. The older the star cluster, the shorter the main sequence of the CMD. From the turn-off point, we can read the total magnitude 'M' of the turn-off stars from the HRD and therefore we will know their age from calculated star models. Since all stars in the star cluster have evolved together from the same cloud of gas, the age of all stars in the cluster is equal. Therefore, when we know the age of a turn-off star in the star cluster, we instantly also know the age of all other stars in the star cluster and therefore also the age of the star cluster itself.

When we plot the magnitudes of all stars of a particular star cluster into a CMD, we will get an 'Isochrone', a line of constant age, since the stars of a star cluster will all have the same age. The Isochrones of different old star clusters will turn-off at different magnitudes. The Isochrones of young star clusters will turn-off at high magnitudes, since the most bright and heavy stars that have the highest magnitudes dye first. When the star cluster becomes older, more and more less heavy stars will turn-off from the main sequence of the CMD. Therefore, the turn-off point is moving downwards to lower magnitudes, the older the star cluster become. The Isochrones of different old star clusters can be plotted into the same CMD giving a field of Isochrones that can be used to categorize and determine the age of a new and unknown star cluster. This is called the 'Isochrone' method to determine the age of open star clusters. The CMD of the new star cluster is plotted over the Isochrone-field and moved upwards until the shape of the CMD is matching one of the Isochrones. The age of the new star cluster can than be read easily from the label of the nearest Isochrone that matches the CMD of the new star cluster the best.

7 Spectroscopy

Spectroscopy is another major technique of astronomy. The spectra of stars can reveal the temperature, chemical composition and physical conditions inside the atmospheres of the stars. Usually a number of absorption lines can be detected that are characteristical for certain chemical elements. The lines are a kind of fingerprint for the chemical compositions and for the classification of stars.
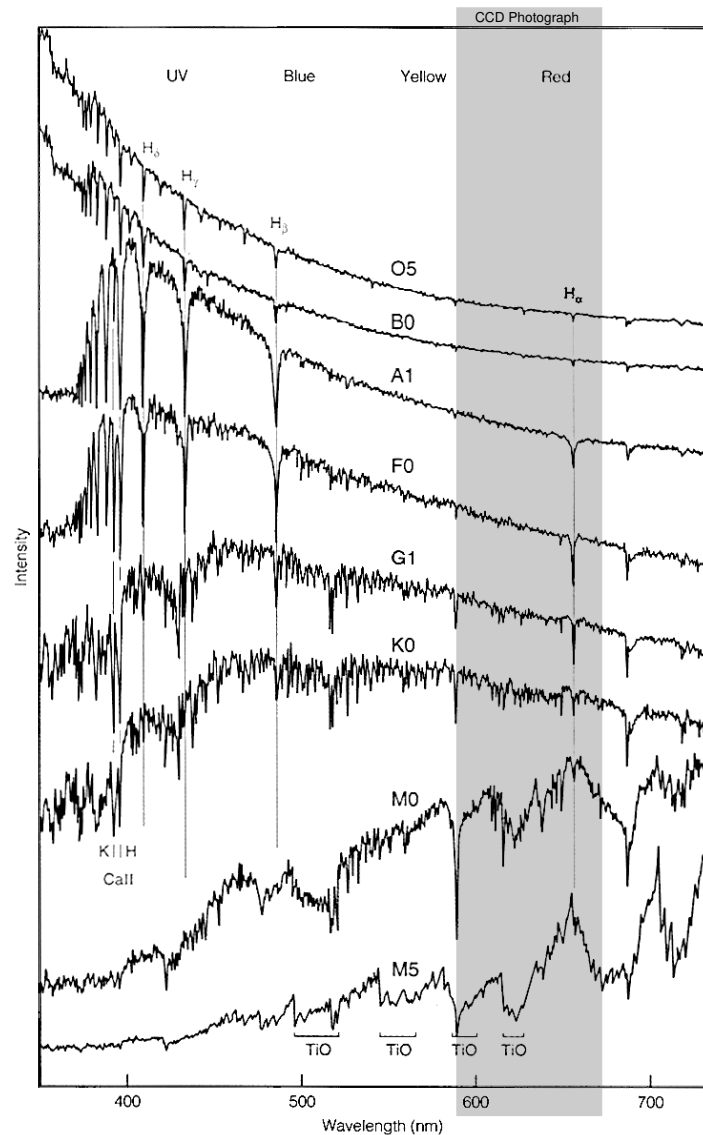

Figure 26: Spectra of different types of stars. The lines indicate the presence of different elements in the atmospheres of the stars. The gray shaded area refers to the range of the photograph shown in Figure 21. Compare the A1 star to the spectrum in Figure 21.

7.1 Star Classification

The comparison of observed spectra with theoretical spectra allows the classification of stars in the HRD when their distance is known. New stars can be easily compared and matched to the HRD classifications in order to determine their physical parameters. For classification, the system of Morgan and Keenan is used that has a two parameter classification, the **'spectral class'** and the **'luminosity class'**.

Table 2: luminosity classes, (Credit: UTK)

Class	Description	Examples
Ia	Bright Supergiants	Deneb (A2Ia)
Ib	Supergiants	Antares (M1Ib)
II	Bright Giants	Canopus (F0II)
III	Giants	Capella (G5III)
IV	Subgiants	Beta Cru (B0IV)
V	Main Sequence	Vega (A0V)

Two parameters are necessary because the classification in the HRD by the 'spectral class' alone is not unique. Giant stars at the end of their lifetime outside the main sequence can still have the same 'spectral class' like main sequence stars although they have tremendous different sizes. For instance, a red giant star can have the same 'spectral class' as a yellow main sequence star. Therefore, a second parameter, the 'luminosity class' was introduced that makes the classification unambiguous. Only when labeling both, the 'spectral class' and 'luminosity class', the star is fully specified. Figure 27 shows the HRD for such a fully classification. On the x-axis are the temperatures, respectively the color index (B-V) of the stars, where the y-axis indicates their magnitudes 'M'. The most dominant feature of the HRD is the S-shaped 'main sequence' that represents the stars during their prime lifetime, while HRD regions outside the 'main sequence' refer to stars at the end of their lifetimes.

The **'spectral class'** is labeled by capital letters 'O', 'B', 'A', 'F', 'G', 'K' and 'M' (Oh Be A Fine Girl/Guy Kiss Me), where each class has ten sub-classes labeled by numbers between '0' and '9'. Recently, two additional spectral classes 'L' and 'T' were introduced for very red objects. Any star can be classified into a 'spectral class' by measuring the strength of different spectral lines and the 'spectral class' is a direct measure for the effective temperature of the star. The thermodynamically stable stellar plasma below the photosphere creates a continuous black-body spectrum that peaks at the effective temperature and defines the main spectral class of a particular star, while the absorption processes inside of the photosphere are generating the spectral features and absorption lines that can be seen in the spectrum of the stars. The temperature of the photosphere decreases from inside out by radiating energy into space. In the outer layers of the photosphere different elements will absorb the light from the stellar interior depending on
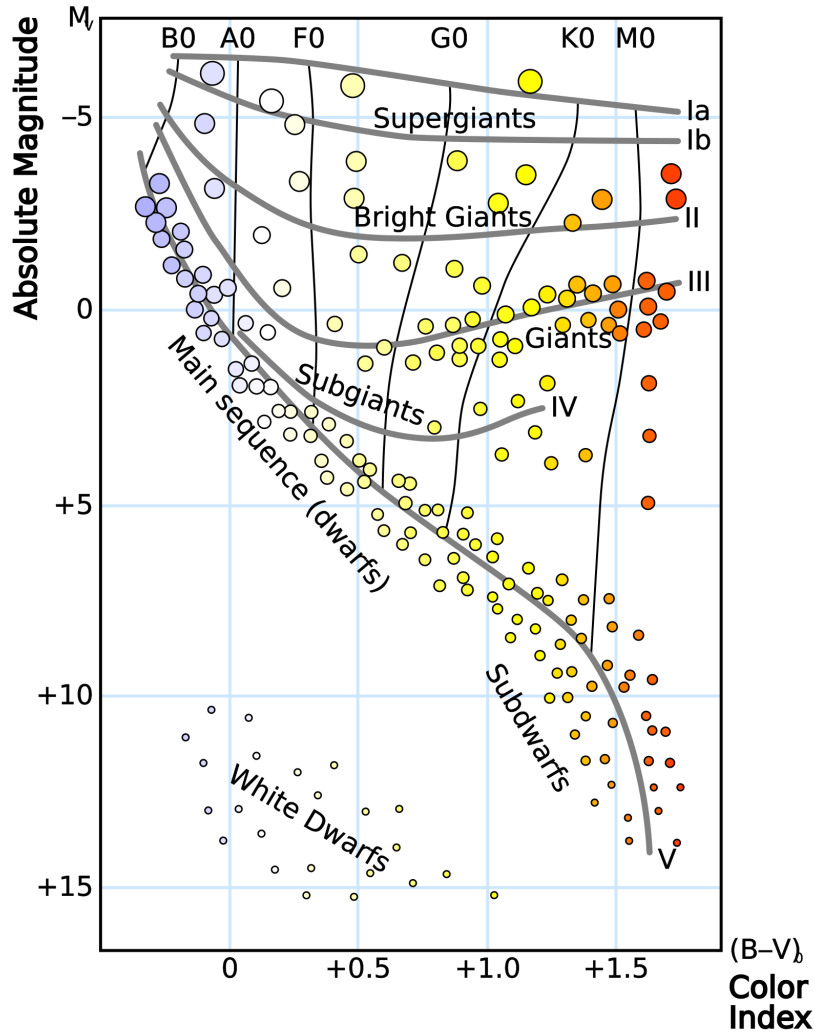
Figure 27: HRD diagram and luminosity classes, (Credit: Wikipedia, Rursus)

the specific type of element and the varying temperatures in the photosphere. Therefore, spectral features are highly depending on temperatures.

> Exercise 5: Which effective temperature of a star corresponds to the spec-
> tral class B, which temperature corresponds to class M? What is the
> spectral class of the sun?

Figure 28 shows the dependencies of the strength of absorption lines and temperature. Hydrogen lines 'H' are peaking for A0 stars at temperatures of around 10000 Kelvin and become fainter on both sides at higher and lower temperatures. Calcium lines 'Ca' grow significant for G type stars and become more dominant as star becomes cooler. At different temperatures, other materials or metals (in stellar spectroscopy all materials beyond
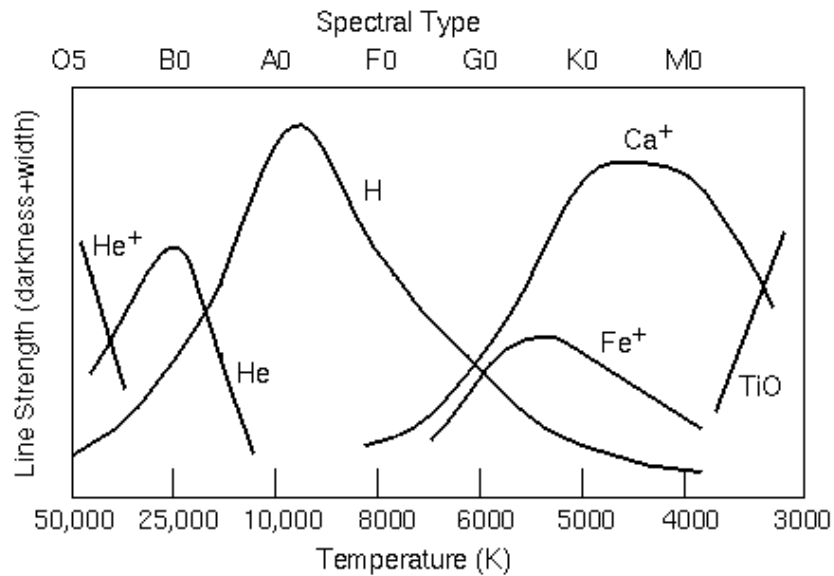
Figure 28: Line strength and temperature dependency, (Credit: astronomynotes.com)

hydrogen are called metals) become the dominant absorbed in stellar atmospheres.

The **'luminosity class'** (from I: 'super giant stars' to V: 'dwarf stars') corresponds to horizontal and diagonal bands in the HRD that are related to the size of the stars, it is also correlated to the width of spectral lines of the stars. For one and the same 'spectral class', the line width of the Balmer series is decreasing with the decreasing 'luminosity class' of the stars. The width of spectral lines depends on the gravitational forces and varies with the mass and the size of the stars. Table 2 gives an overview of the 'luminosity classes'.

Figure 26 shows the spectra of a number of different sized stars, meaning stars of different spectral classes. Most spectral features are found in the UV, a good reason why spectroscopy is much more popular in UV astronomy than imaging. A very popular feature in the spectrum are usually the H_α, H_β, H_γ, H_δ lines of the Balmer series that are caused by ionized hydrogen that is the most abundant material in the stars atmospheres.

8 Experiment and Data Analysis

For the experimental part, the 80 cm telescope of the IAAT at Sand 1 will be used. The tutor of the lab course will introduce and instruct you into the function of the telescope and will help you with the operation of the instruments during the observation night. We will photograph a BLUE and a GREEN image of an open star cluster with the STL1001 CCD photometric star camera and also take the Spectral-Image of a star using the 10C spectrograph and its CCD camera. If the weather does not permit any observations, we will still give you an introduction to the observatory and use some data files from an earlier observation.
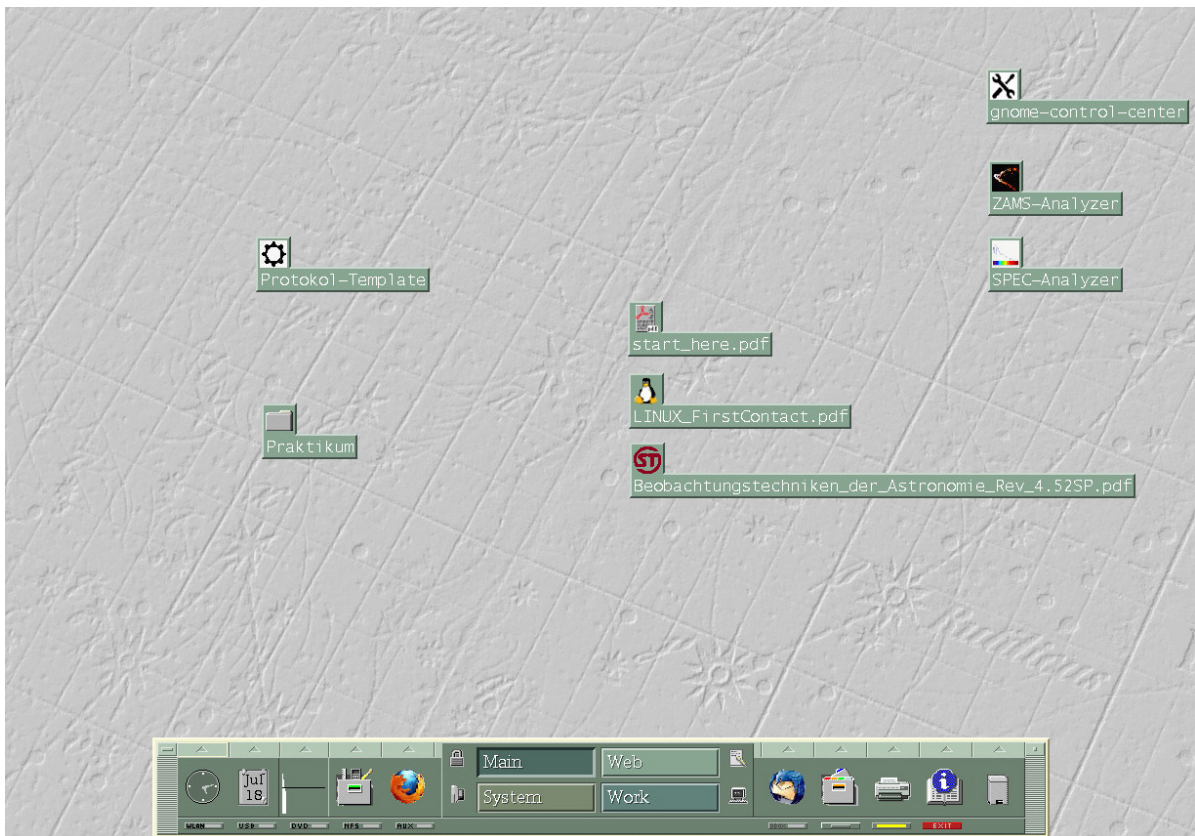
Figure 29: 'astro' login on the lab course laptop computer

For the data analysis part, you will analyze the recorded data on a laptop computer that the IAAT will loan you temporary. Instructions for data analysis you will find in this chapter. The analysis is based on IDL[5] scripts and performed by two applications, the '**ZAMS-Analyzer**' and the '**SPEC-Analyzer**' that are both installed on the lab course laptop computers. Both scripts will guide you in a step by step procedure interactively through the analysis, double click the left mouse button onto it in order to launch

---

[5]Interactive Data Language

it. There are also two videos 'Howto_Spectroscopy.m4v' and 'Howto_Photometry.m4v' installed on the laptop computer that are giving you an example of how to perform the data analysis. Start the videos in the '~/Praktikum/PhotometrySpectroscopy/Videos/' subfolder, just by clicking the left mouse button twice onto the video file. You can run the Howto_Spectroscopy.m4v and Howto_Photometry.m4v videos also from the IAAT website on an internet webbrowser.
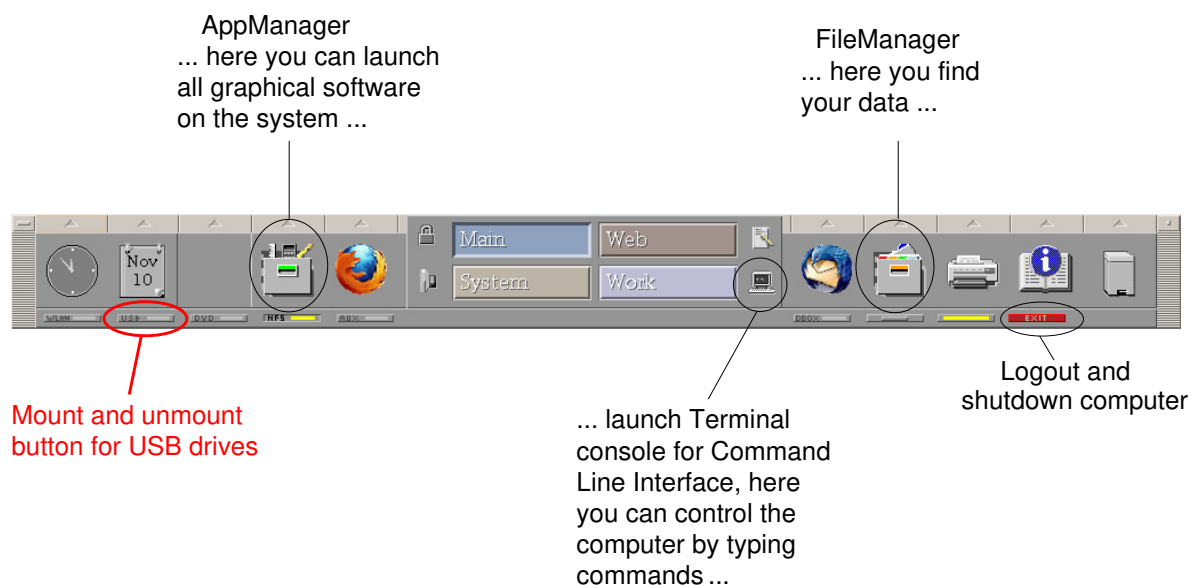
Figure 30: You can mount and unmount USB sticks via the CDE desktop manager.

You can login onto the lab course laptop computer with the account name 'astro' and the password 'astro'. This will open the CDE[6] graphical desktop interface as it is shown in Figure 29, giving you access to your files and to the IDL/GDL analysis software 'ZAMS-Analyzer' and 'SPEC-Analyzer'.

Figure 30 shows the CDE desktop manager console. In order to copy your data from an USB-Stick onto the lab course laptop computer, plug in the USB-Stick to a USB port and press the small 'USB' mount button on the console of the CDE desktop manager. This will mount your USB-Stick and open the 'File-Manager' of CDE. You can copy the data by dragging and dropping the files with the mouse pointer from the USB-Stick folder into the HOME folder of the 'astro' account (~/Praktikum/PhotometrySpectroscopy/Data). If the target folder does not exist, you can create it via the File-Manager menu 'File->NewFolder'. In order to unmount the USB-Stick again, please press the 'USB' mount button a second time and wait until the yellow light in the button goes OFF. Afterwards you can safely remove the USB-Stick from the computer. In order to shutdown the laptop computer, please use the small red 'Exit' button on the CDE desktop manager console.

---

[6]Common Desktop Environment

In order to perform the analysis, the computer needs access to the internet. You can plug in a wired Ethernet cable (RJ45) to the computer and connect it to a locale network that is supporting DHCP[7]. Alternatively, you can also use wireless LAN at some local WLAN network of your choice. In the vicinity of the University Main Campus or at Campus Sand, you can use WLAN with your 'edoroam' account to get access to the internet. Please configure the WLAN access by utilizing the '**gnome-control-center**'- Wi-Fi setup that you find on the Desktop of the computer or in the Application Manager under subfolder 'Config/Network/'. Figure 31 shows a screenshot of the 'eduroam' setup that is required for wireless access to the internet at the University Campus. Notice, that you have to type in your own 'eduroam'-login and password in the field 'Username' and 'Password'.
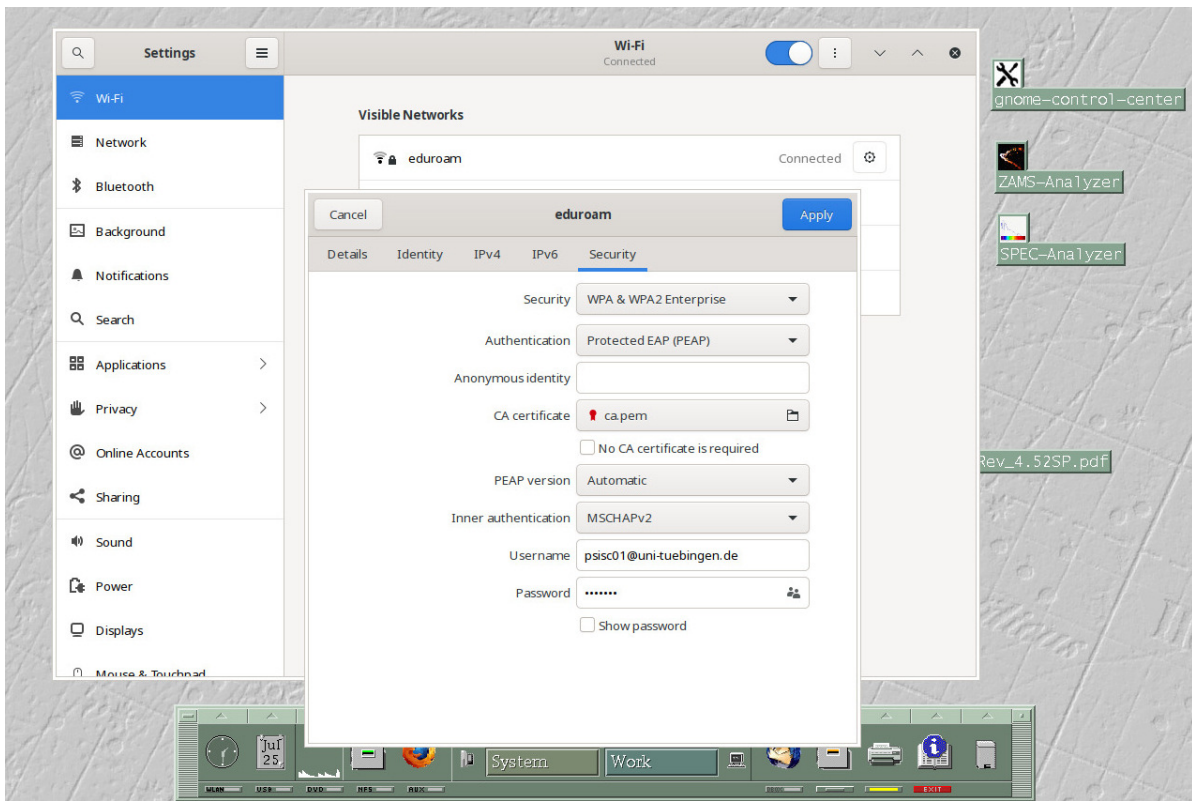

Figure 31: 'eduroam' Wi-Fi configuration via 'gnome-control-center'

8.1 The Photometric Experiment

For the photometric experiment, the CCD camera SBIG STL1001 will be mounted to the left focus of the 80 cm telescope as shown in Figure 32. The camera has a filter wheel

---

[7]Dynamic Host Configuration Protocol

and is controlled by the Maxim-DL software on the Navigation-&Observationcomputer. For the photometric analysis, a BLUE and a GREEN image of an open star cluster will be photographed.

Figure 32: The SBIG STL1001 photometric CCD camera at the left focus of the 80 cm telescope (left). Open star cluster as an observation object for the photometric experiment (right).

Using the BLUE and the GREEN FITS image, we want to generate a Color-Magnitude-Diagram (CMD) and use the Zero-Age-Main-Sequence (ZAMS) to determine the distance and the age of the star cluster. Therefore, we select 5 stars of the cluster and compare the recorded BLUE 'B' values and recorded GREEN 'V' values with literature values from the WEBDA online data base in order to correct for the color filters used during the recording and in order to determine the color of the stars in the cluster. Figure 33 shows the BLUE and GREEN images of a typical star cluster (M35) as they were taken with the STL1001 camera of the 80 cm observatory.

> Exercise 6: Mount the STL1001 CCD camera to the left focus of the 80 cm telescope, slew the telescope to the star cluster you have selected for photometry. Take photographs of the star cluster using the blue and the green filter setting of the STL1001 star camera.

In order to begin the photometric analysis, click onto the ◨-pictogram of the **'ZAMS-Analyzer'** software script. This will open a window that is guiding you interactively through the analysis, just follow the instructions! The script is written in IDL/GDL and a combination of mouse pointer controlled actions and command line inputs. During mouse pointer inputs, it is unforgiving of erratic mouse button clicking even outside the active input windows. In case you accidentally continue or terminating the analysis by mistake, you must start the analysis from the beginning again. Be careful when clicking
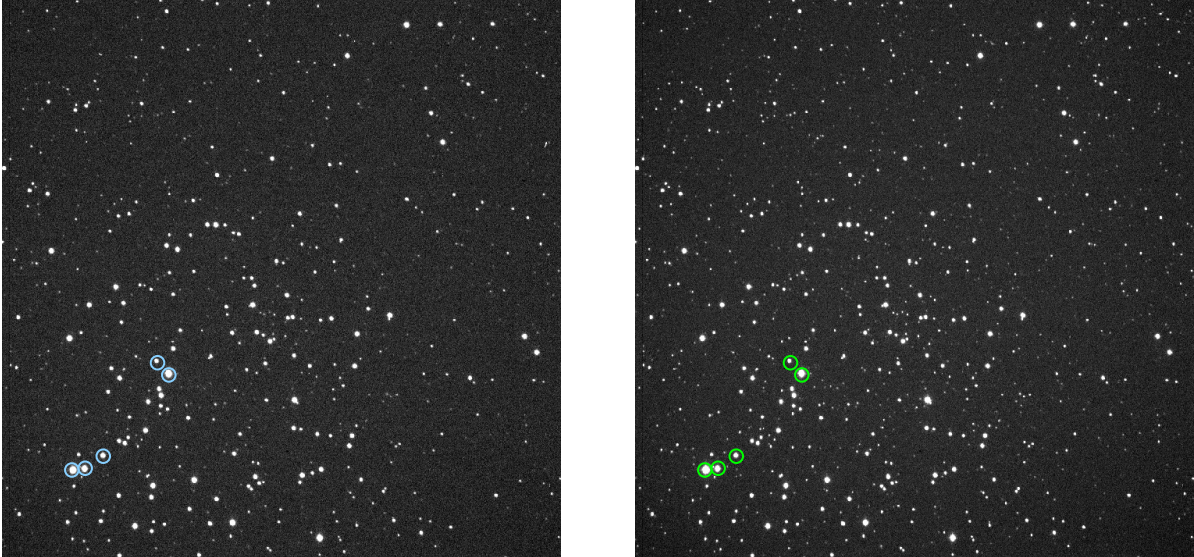
Figure 33: BLUE and GREEN Image of the M35 star cluster taken at the 80 cm observatory of the IAAT. The 5 marked stars were used for color filter calibration.

the mouse buttons, only click as the script is requesting it!

Figure 34 presents a flow chart of the whole photometric analysis procedure as it is guided by the 'ZAMS-Analyzer' software script. In step **(A)**, 5 stars of the star cluster will be chosen for color filter calibration. The color filters used in the observatory for photometry will produce different magnitudes compared to standard filters. Therefore, the magnitudes for 'B' and 'V' of the recorded BLUE and GREEN FITS images must be compared to literature values that are listed on the WEBDA data base (https://webda.physics.muni.cz/navigation.html) for correction. For the 5 chosen stars, the standard values for 'B' and 'V' must be noted from the WEBDA data base. They will be compared to the 'B' and 'V' values that are processed from the recorded BLUE and GREEN FITS images in step **(B)** and step **(C)** by the analysis script. Following, correction values for 'B' and 'V' must be calculated manually and then input to the 'ZAMS-Analyzer' software script that will color correct the recorded BLUE and GREEN FITS images in step **(D)** of the script.

In step **(E)**, the star positions of the recorded BLUE and GREEN images will be aligned to each other. For this, one and the same star must be chosen and input to the software script in both images (BLUE and GREEN) by pointing the mouse pointer onto the same star and clicking the left mouse button to register it. The IDL/GDL software than will move the GREEN image in x- and y-direction as long as the star positions are exactly matching the star positions in the BLUE image.

Following Figure 34, step **(F)** will generate a Color-Magnitude-Diagram (CMD) of the star cluster. The stars that shall be considered for the CMD must be selected manually.
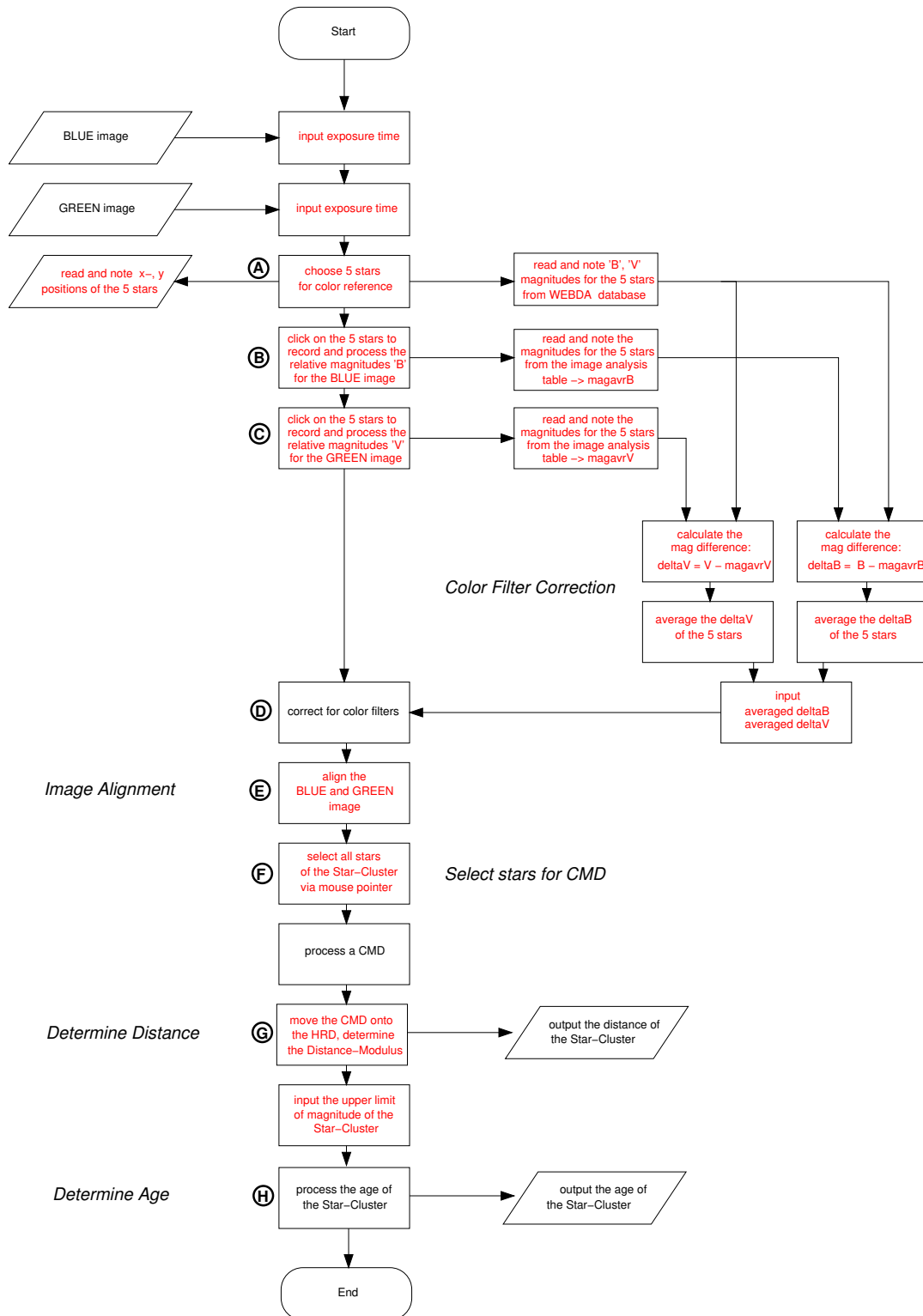
Figure 34: Flow Chart of the photometric analysis. The red steps require a manual action or input

Therefore, select all stars in FITS image (GDL 0) by using the mouse pointer star by star and click the left mouse button for registering. Select as many stars as you can, the more stars you register the better the CMD will be! If you think a particular star in the field is a foreground star and does not belong to the star cluster, than do not register it. If you select a particular star more than once by accident, just continue, it will not harm the generation of the CMD. You should select at least 30 to 40 stars, more is better. When you have completed the selection, than press the right mouse button to close the selection. During the selection phase, do not click on any other window or application on the screen and by all means, do only click the right mouse button when you want to close the selection! After completing the input, the 'ZAMS-Analyzer' script will plot a CMD of the star cluster as shown in Figure 35.
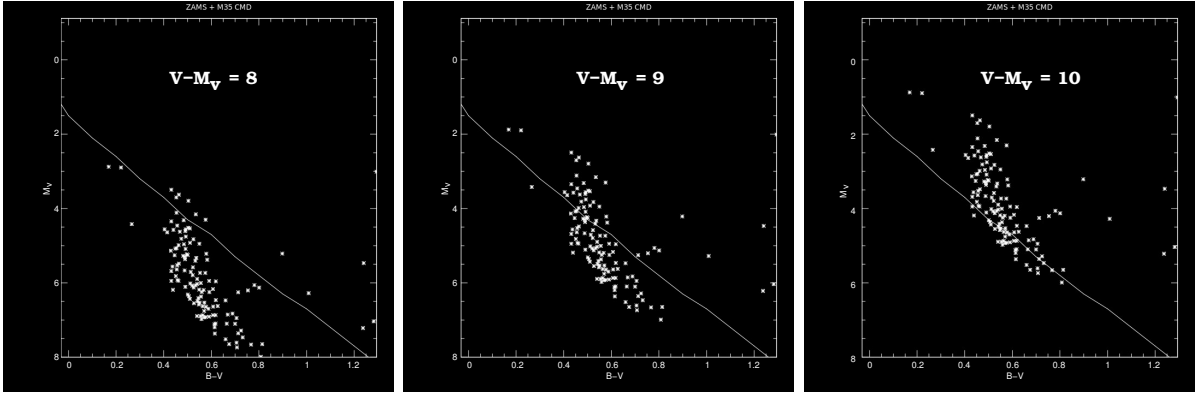
Figure 35: The CMD is represented by the cloud of white dots, the HRD is the continuous white line. In order to align the CMD to the HRD, the CMD must be moved upwards the HRD until it only touches the HRD with its lower edge. The optimum approximation is reached at a Distance-Modulus $(V - M_v)$ of about 10, here in this example.

In step **(G)**, the CMD will successively moved upwards the HRD, and the Distance-Modulus '$(m - M)$' at the perfect match is determined. The relative magnitude 'm' is considered to match the measured magnitudes 'V' of the GREEN image, leading the Distance-Modulus into '$(V - M_v)$' for simplification that transforms Equation 17 into Equation 19.

$$(V - M_v) = 5 \, log(r) - 5 - A_\nu \tag{19}$$

For the iteration, a first value for $(V - M_v)$ is input to the script and than improved more and more until the CMD is adapted to the HRD. At the best approximation, the distance of the star cluster to Earth is output by the 'ZAMS-Analyzer' software script. Figure 35 shows such a sequence of approximation. The CMD is represented by a cloud of white dots that are the magnitudes of the individual stars in the star cluster, the continuous line in between is the main sequence of the HRD. The left image shows the

CMD at a Distance-Modulus $(V - M_v) = 8$, the middle image has a Distance-Modulus $(V - M_v) = 9$ and the right image a Distance-Modulus $(V - M_v) = 10$, which is the optimum approximation. At optimum approximation, the CMD must be moved above the HRD as shown in the right image of Figure 35, where only the lower edge of the CMD touches the HRD.

Finally, the age of the star cluster can be determined in step **(H)** of the software script by using the 'Turn-Off' method. Since all stars inside a star cluster usually develop together, the age of the star cluster can be determined when finding out the age of a particular star inside the cluster. This can be done by the most massive bright stars in the star cluster. Since the most bright stars reach their end of lifetime ahead of all other stars and turn-off from the main sequence, they can be identified from the CMD/HRD as a branch perpendicular to the main sequence. Observing the stars in the CMD, we look for stars that are turn-off from the main sequence at the highest magnitude values of the star cluster and then use this absolute magnitude value 'M_v' as an input for the age determination. From this turn-off value, the 'ZAMS-Analyzer' software script will calculate the age of the star cluster as an output value. In Figure 35, the turn-off value for the age determination would be somewhere between 'M_v' = 1 and 'M_v' = 1.5 magnitude.

Alternatively, a second method for step **(H)**, the 'Isochrone' method can be used. At the 'Isochrone' method, the CMD will be moved over a field of Isochrones until the shape of the CMD is fitting the field of Isochrones best. At the best approximation, the age of the star cluster can be read simply from the label of the nearest 'Isochrone' line.

There is a video 'Howto_Photometry.m4v' on the lab course laptop computer that shows an example how to perform the photometric analysis.

> Exercise 7: Describe the photometric analysis. What do you see in the
> CMD? How far is the star cluster away from Earth? How old is the
> star cluster? Compare your results to literature data and discuss where
> differences come from?

8.2 The Spectroscopic Experiment

For the spectroscopy experiment, the 10C spectrograph will be mounted to the left focus of the 80 cm telescope as shown in Figure 36. The spectrograph has a CCD camera that photographs the 'Spectral Image' of the star and is controlled by the Maxim-DL software on the Navigation-&Observationcomputer. For the spectroscopic experiment the 'Spectral Image' of a star will be photographed.

In this section we want to analyze a spectral-FITS-image that was recorded with the 10C spectrograph of the observatory and is shown in Figure 37. In order to launch the spectral analysis, click on the -pictogram of the **'SPEC-Analyzer'** software script.

Figure 36: The 10C spectrograph mounted at the left focus of the 80 cm telescope (left). The CCD camera of the spectrograph will photograph a spectral image that is required for the spectral analysis (right).

This will open a window that is guiding you interactively through the analysis, just follow the instructions! The script is written in 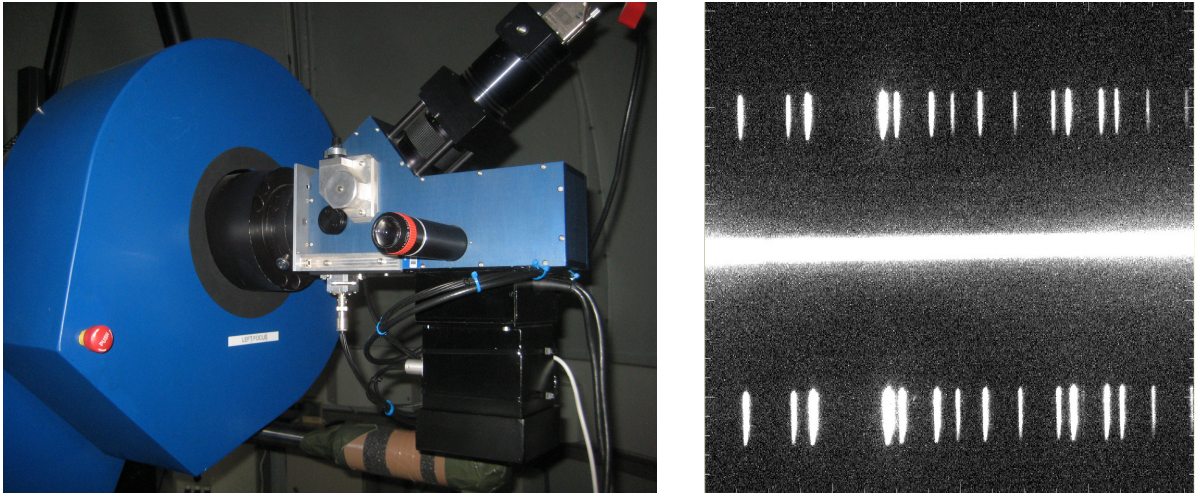IDL/GDL and a combination of mouse pointer controlled actions and command line inputs. During mouse pointer inputs, it is unforgiving of erratic mouse button clicking even outside the active input windows. In case you accidentally continue the processing by mistake, you must terminate the analysis and start from the beginning again. Be careful when clicking the mouse buttons, only click as the script is requesting it!

> Exercise 8: Set the spectral gear setting of the 10C spectrograph to the value of 14. Mount the 10C spectrograph to the left focus of the 80 cm telescope and slew the telescope to the position of the star you have selected for spectroscopy. Take a spectral-image of the star with the CCD camera of the spectrograph for spectroanalysis.

Figure 37 shows the spectral-image of the star Vega in constellation Lyra. The photograph was taken at the spectrographs spectral order gear setting of 14 that only covers a small part of the full optical spectral range from setting 10 (4000 Å) to setting 19 (8000 Å). For the lab course, the spectral order gear is usually chosen to a setting that covers the most prominent hydrogen H_α absorption line that is dominant in star atmospheres and it is limited to only one single photograph for simplicity. In order to record a full optical spectrum, about 10 spectral-images like Figure 37 would be required at different spectrograph settings and to be assembled to a full range spectral-image by using imaging software first, before a spectral analysis can be applied and performed. Figure 20 shows the full range optical spectral-image together with the smaller range of the spectral-image (gray column) as it is usually taken on the lab course observation day.
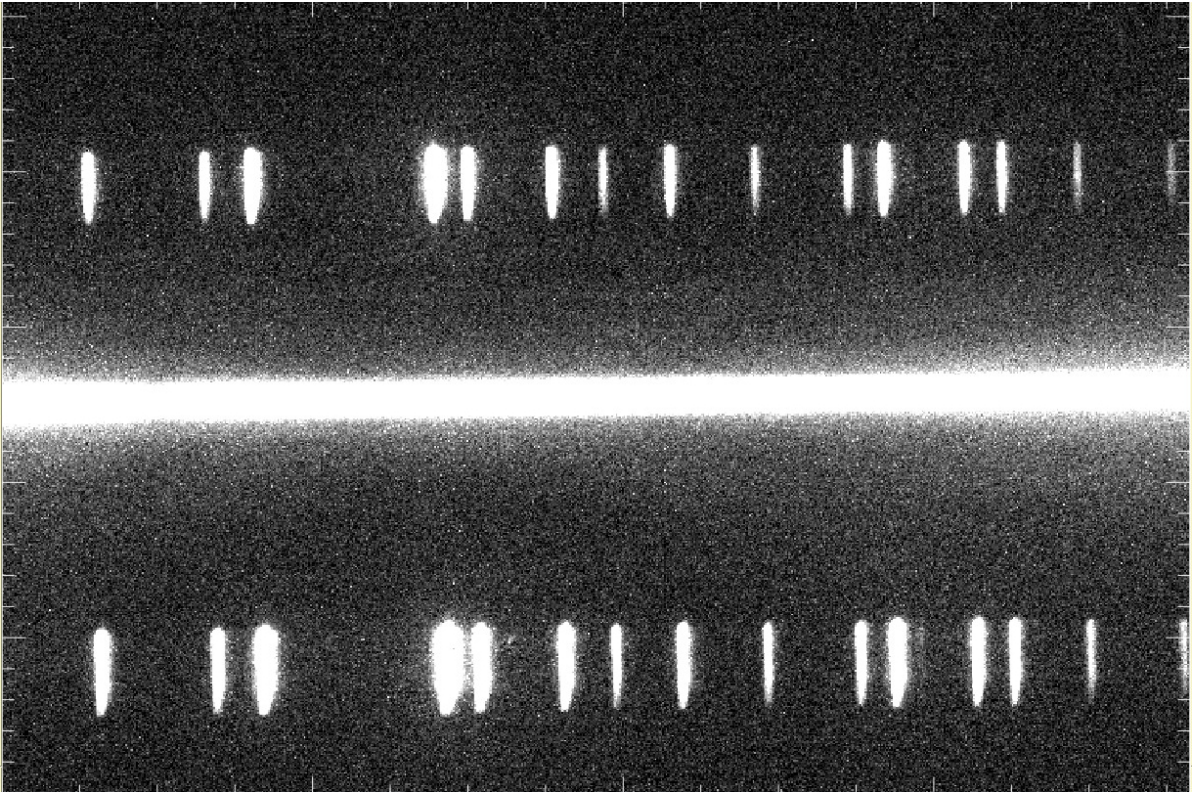
Figure 37: The Figure shows a spectral-image that was recorded by the 10C spectrograph of the observatory at a spectrograph setting of 14. The bright band in the middle contains the spectrum of the star, spectral features can only be resolved by further spectro analysis.

The spectral lines in the upper and lower part of Figure 37 are generated by the Neon- and Mercury lamps of the spectrograph and will be used for calibration later. Between this calibration lines, the spectrum of the star is appearing as a bright horizontal band in the middle of the image. Brightness variations and absorption features inside this bright horizontal band usually can not be resolved by the naked eye without the use of sophisticated photometric techniques. The spectrum of the star can be unveiled only by spectral analysis.

The whole procedure of spectral analysis, guided by the 'SPEC-Analyzer' software script is shown in the flow chart presented in Figure 38. The spectral-image is used as an input to the 'SPEC-Analyzer' software script and displayed onto the computer screen in stage **(A)**. In order to extract a spectrum, the 'SPEC-Analyzer' software script will scan **'Traces'** from the spectral-image, which are basically one dimensional IDL arrays that contain the gray levels of all pixels along the x-axis, for different y-positions of the spectral-image. Altogether, there will be three Traces required: **'cal-trace1'**, that contains the pixels of the calibration lines in the lower part of Figure 39 (y = 81), **'cal-trace2'**, that contains the pixels of the calibration lines in the upper part of Figure 39 (y = 364), and **'spec-trace'** that includes the pixels in the bright band in the middle

53

Figure 38: Flow Chart of the spectral analysis. The red steps require a manual action or input

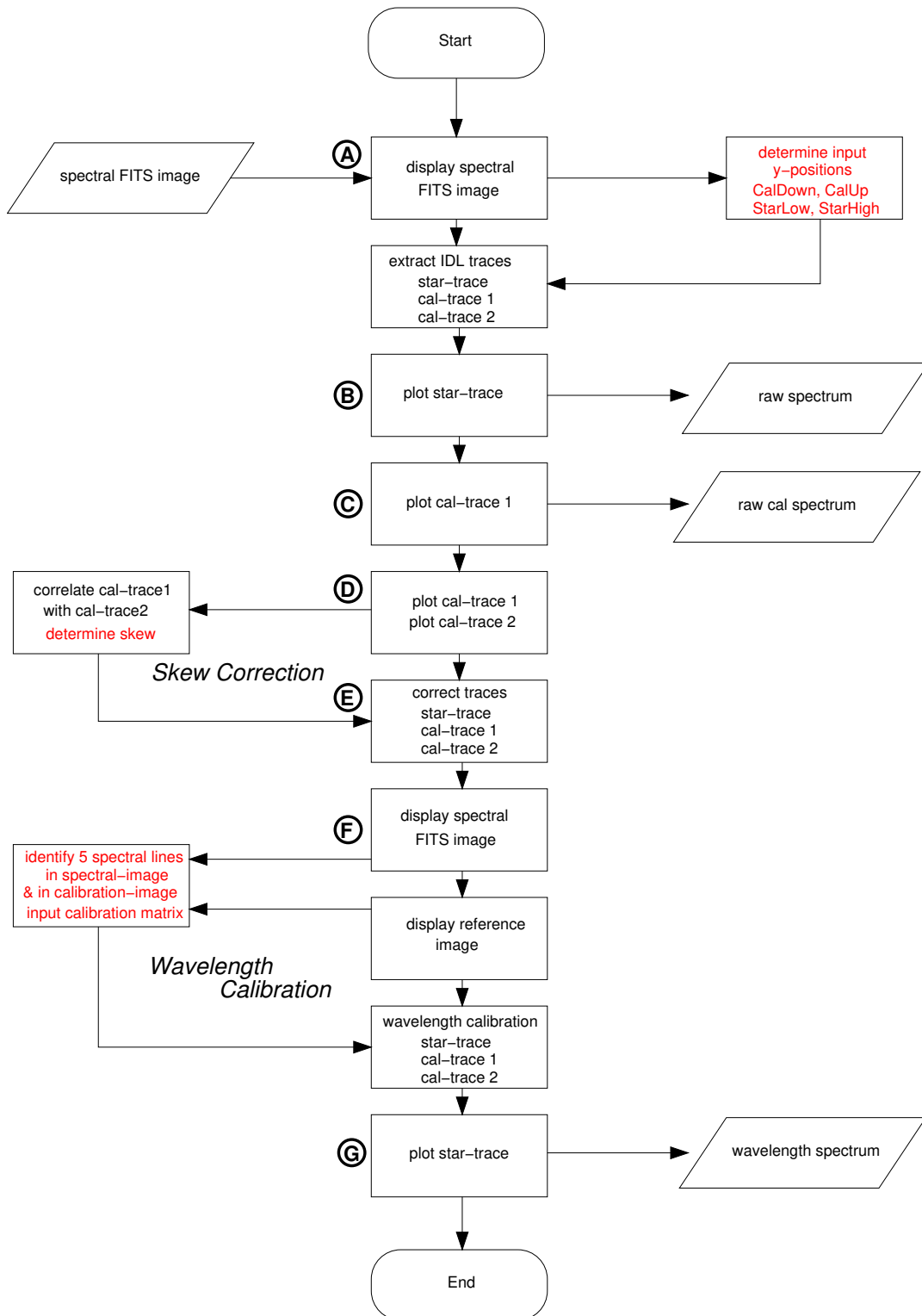part of the spectral-image (y = 254 to y = 260). Actually, 'spec-trace' is not made from a single trace like 'cal-trace1' and 'cal-trace2', but rather generated by the average of a larger number of traces along the x-axis by the 'SPEC-Analyzer' software script for a small range of different y-positions that covers the starlight spectrum. Figure 39 illustrates the idea of the Traces. The y-positions, where to take such traces, must be determined manually by the user and then input to the 'SPEC-Analyzer' software script.
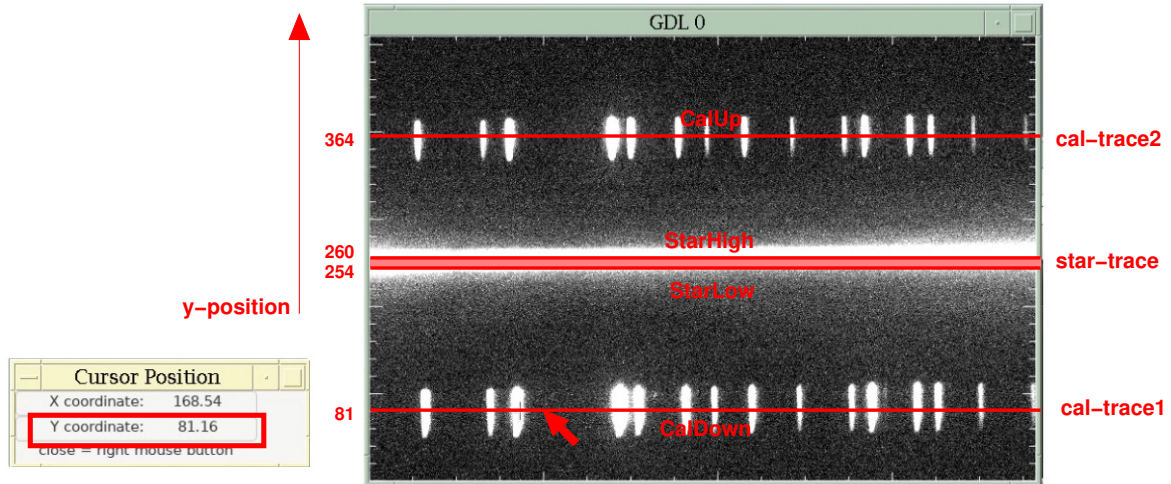
Figure 39: Spectral-image and y-positions 'CalDown' for **'cal-trace1'**, 'CalUp' for **'cal-trace2'**, as well as the y-positions 'StarLow' and 'StarHigh' for **'spec-trace'**. Choose the y-position values in a way, that the horizontal trace line stays inside the corresponding light spectra over the complete x-axis range. Read the mouse pointer y-position from the IDL 'Cursor Position' tool.

Step **(B)** of the 'SPEC-Analyzer' software script is plotting the **raw spectrum** of the star that is contained in 'spec-trace'. It shows the light intensity over the pixel number in x-direction and is not calibrated to wavelength units yet. Step **(C)** is plotting the content of the trace 'cal-trace1' respectively, that contains the raw calibration spectrum of the Neon- and Mercury-lamps.

Since the CCD camera is removable, the image plane of the CCD and therefore the spectral-image can be rotated relative to the x-axis of the spectrograph, resulting in a skew between the spectral-image and the trace-axis. This skew can be determined and compensated by correlating the two calibration traces 'cal-trace1' and 'cal-trace2' with each other. The value of maximum correlation can be determined manually and be used as an input to the 'SPEC-Analyzer' software script for correction. The correlation is performed in step **(D)** and the skew correction in step **(E)** of the 'SPEC-Analyzer' software script, also shown in Figure 38.
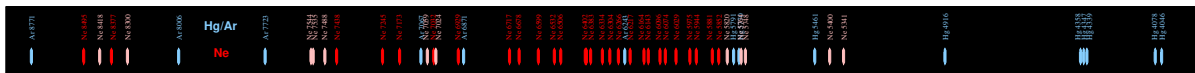
Figure 40: Calibrated-spectral-image as it is used as a reference for wavelength calibration. The calibrated-spectral-image contains all spectral lines of the Neon- and Mercury lamps that are labeled with their corresponding wavelength numbers. A calibration matrix can be generated just by comparing the spectral-image of Figure 37 to the calibrated-spectral-image that is shown here.

In order to perform a wavelength calibration, the skew corrected spectra in 'cal-trace1' and 'cal-trace2' can be compared to a reference spectrum that contains the same calibration lines as 'cal-trace1', 'cal-trace2' but is labeled with wavelength numbers instead of pixel numbers. Such a reference spectrum can be obtained from literature. For the lab course however, we will use a calibrated-spectral-image rather than a plotted spectrum for identification, since the compare of the recorded spectral-image to a calibrated-spectral-image is much easier than to a plotted spectrum. The calibrated-spectral-image used for the lab course is shown in Figure 40, it was recorded earlier from the calibration lamps of the 10C spectrograph and labeled with wavelength numbers for the whole optical range from 4000 Å to 8000 Å.

In step **(F)** of the spectral analysis, we manually compare the spectral-image of Figure 37 to the calibrated-spectral-image shown in Figure 40 or to the matching part of it (use the zoom menu of the ghostview (gv) software to scale the calibrated-spectral-image accordingly). Following, we input a calibration matrix for 5 spectral lines we have arbitrary chosen from the spectral-image. The calibration matrix does contain 5 number doubles that connect pixel numbers to wavelength numbers. The calibration matrix will be applied by the 'SPEC-Analyzer' software script to the traces 'cal-trace1', 'cal-trace2' and 'spec-trace', converting the pixel numbers into wavelength numbers. Finally, the calibrated spectrum in 'spec-trace' can be plotted during step **(G)** again, and the spectral analysis script is terminated.

Figure 41 is the final output of the spectral analysis. The plot shows the intensity of light on the y-axis against the wavelength numbers on the x-axis. Comparing the spectrum-plot of Figure 41 to the spectral-image of Figure 37 shows a tremendous gain in information about the spectral brightness distribution along the x-axis. The large dip in the spectrum-plot of Figure 41 at 6600 Å is the H_α absorption line of the stars atmosphere. Other spectral features are weaker and also different for different types of stars. Please consult the 'Atomic Spectra Database (ADS)' of the 'National Institute Of Standards And Technology' at (https://physics.nist.gov/PhysRefData/ASD/lines_form.html) for an overview of all known spectral lines and in order to clarify the occurrence of certain spectral lines in the spectrum of the recorded star.

There is a video 'Howto_Spectroscopy.m4v' on the lab course laptop computer that shows you an example how to perform the spectral analysis.
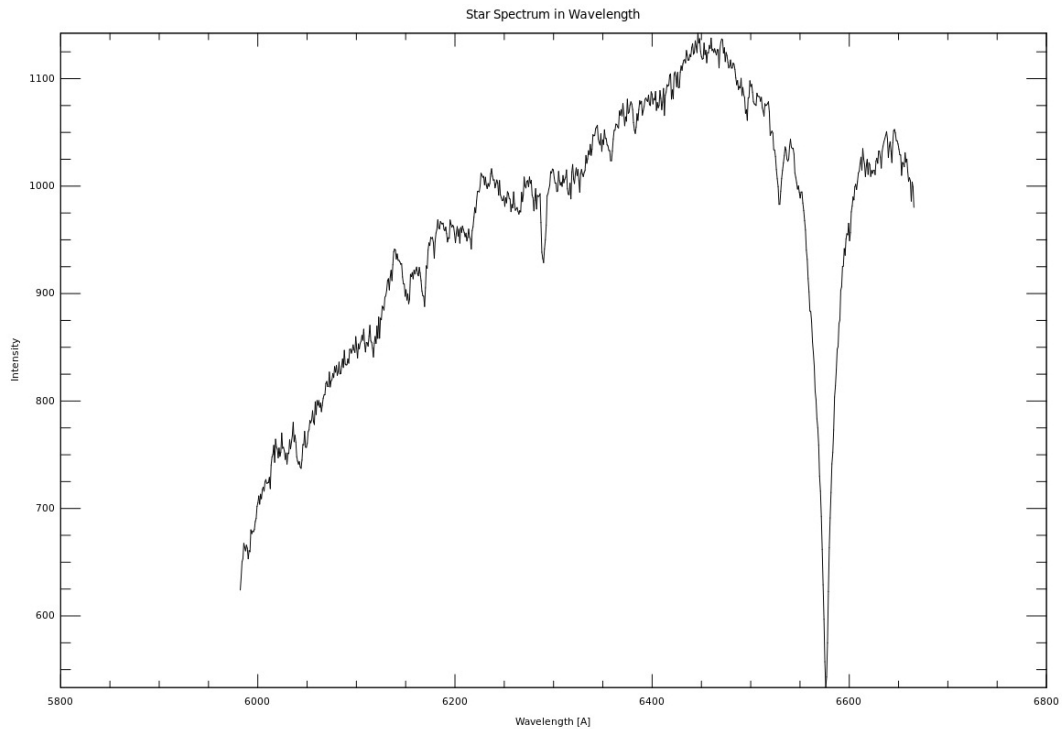
Figure 41: The final product of the spectral analysis is the here presented spectrum-plot. Features in the spectrum can be caused either by absorption in the stars atmosphere, by interstellar medium or even by molecules inside the Earth atmosphere. A discussion of the spectral features is expected to be part of the lab course protocol.

> Exercise 9: Referring to the print outs, describe how the spectral analysis has been performed? What is the spectral class of the observed star? What is the physical difference between the calibration lamp spectra and the stellar spectrum you have recorded? Why do we see absorption lines in the stellar spectrum but emission lines in the calibration spectrum? What information can be extracted from the stellar spectrum?

9 The Protocol

For the Offline Data Processing we will loan you a Laptop Computer. The Laptop Computer runs the LINUX operation system and includes all necessary software needed for data analysis as it is described in this manual. The 'Username' for the Laptop Computer is 'astro', the password is also 'astro'. You can produce all necessary plots for the protocol on the Laptop Computer using the 'ZAMS-Analyzer' and 'SPEC-Analyzer' software scripts. Please return the Laptop Computer after you have submitted the protocol to the institute again (IAAT, Sand 1, EG, Office A107)!

Please follow the guidelines for the Protocol handed out at the beginning of the lab

course! The Protocol should include at minimum:

- (A) An introduction into the purpose of the experiment

- (B) A brief chapter about the theory of the telescope, the CCD camera as well as the photometric and spectroscopic techniques.

- (C) What star cluster was observed and recorded? What distance and age was determined by the photometric analysis? Discuss reasons for the deviation from literature data.

- (D) What star was spectro-analysed? What can we learn from the recorded spectrum?

- (E) Concluding remarks to the experiment

The Protocol should be in size between 10 and 50 pages. It must be your own work!. We will not accept copy and paste text from other protocols, from the Course Manual, from Wikipedia or from other sources. If you make use of pictures or figures from other sources you must clearly reference its origin and its copyright holder!

We recommend clearly the 'LaTeX' document writing system as the best tool to produce professional protocols, papers or any other scientific or technical documentation. LaTeX is open source and free to download for any existing operating system! There is a LaTeX template for the protocol also on the Laptop Computer. If you want to write the protocol in LaTeX you can use this template and the LaTeX system already installed on the Laptop Computer for this purpose. You will find the protocol template in the folder 'Rraktikum/Protocol_LaTeX-Template' on the Laptop Computer. Just start the File Manager, navigate to the folder and double click the left mouse button on the file 'Protocol.TEX' This will start an Integrated Development Environment for the LaTeX system. On the left side of the computer screen it will display the LaTeX source code you can modify and edit for your purpose, on the right side of the computer screen you can see the document results after compiling. The LaTeX compiler will finally produce a 'pdf'-Document.

We accept protocols produced by any other document writing system also, as long as it fulfills some certain criteria of scientific documents:

- Titel Page, Date of origin, Author, Group Number

- Paragraphs/Chapters

- Table of contend

- Numbered pages

- Numbered figures, tables or equations

- Figures with subtitels, tables with upper text

- References

Please return the Laptop Computer after you have submitted the protocol to the institute again (IAAT, Sand 1, EG, Office A107), thank you!

10 Appendix A: Celestial Objects

Table 3: list of celestial objects for observation

name	type	R.A. [HH:MM:SS]	DEC [Deg:Min:Sec]
M11	open star cluster		
M34	open star cluster		
M36	open star cluster		
M39	open star cluster		
10 Lac	star		
α Cam	star		
α Cas	star		
β Cas	star		
γ Cas	star		
β Dra	star		
α Lyr	star		
η Uma	star		

11 Appendix B: Wavelength Calibration

Table 4: literature wavelength of the Neon- and Mercury lamps from Kurucz (http://cfa-www.harvard.edu/amdata/ampdata/kurucz23/sekur.html)

Ion	$\lambda[\text{Å}]$	Ion	$\lambda[\text{Å}]$	Ion	$\lambda[\text{Å}]$
Hg I	4046.559	Hg I	5790.660	Ne I	6266.495
Hg I	4077.827	Ne I	5852.488	Ne I	6304.789
Ne I	4314.252	Ne I	5881.895	Ne I	6334.428
Hg I	4358.323	Ne I	5944.834	Ne I	6382.991
Hg I	4916.062	Ne I	5975.534	Ne I	6402.246
Ne I	5116.503	Ne I	6029.997	Ne I	6506.528
Ne I	5330.777	Ne I	6074.338	Ne I	6532.882
Ne I	5341.094	Ne I	6096.163	Ne I	6598.953
Ne I	5400.562	Ne I	6143.062	Ne I	6678.331
Hg I	5460.731	Ne I	6163.594	Ne I	6717.043
Hg I	5769.593	Ne I	6217.281		

12 Appendix C: Prominent lines in stellar spectra

Table 5: Hydrogen

H_α	H_β	H_γ	H_δ	H_ϵ	H_ζ	H_η	H_θ
6563 Å	4861 Å	4340 Å	4102 Å	3970 Å	3889 Å	3835 Å	3798 Å

H_ι	H_κ	H_{13}	H_{14}	H_{15}	H_{16}	H_{17}	H_{18}
3771 Å	3750 Å	3734 Å	3722 Å	3712 Å	3704 Å	3697 Å	3692 Å

Table 6: Helium

He I	3820 Å	3965 Å	4009 Å	4026 Å	4144 Å
He I	4387 Å	4471 Å	5876 Å		
He II	3923 Å	4100 Å	4199 Å	4340 Å	4542 Å
He II	4686 Å	4861 Å	5411 Å	6678 Å	

Table 7: Carbon

C II	4267 Å						
C III	4069 Å	4123 Å	4187 Å	4340 Å	4375 Å	4515 Å	4650 Å
C IV	4441 Å	4650 Å	4786 Å				

Table 8: Nitrogen

N II	3995 Å	5005 Å	5679 Å
N III	4100 Å	4640 Å	
N IV	4057 Å		

Table 9: Oxygen

O I	6158 Å							
O II	3749 Å	4119 Å	4317 Å	4320 Å	4349 Å	4415 Å	4417 Å	4649 Å
O III	3444 Å	3760 Å	4069 Å					
O IV	4786 Å							
O V	4123 Å	4157 Å	4187 Å					

Table 10: Sodium

Na I	5890 Å	5896 Å

Table 11: Silicon

Si II	4128 Å	4130 Å
Si III	4552 Å	
Si IV	4089 Å	

Table 12: Calcium

Ca I	4227 Å	4289 Å	4303 Å	4435 Å	4455 Å	5016 Å	5262 Å
Ca I	5270 Å	5589 Å	5857 Å	6122 Å	6439 Å	6718 Å	
Ca II	3934 Å	3968 Å					

Table 13: Iron

Fe I	3930 Å	4005 Å	4045 Å	4064 Å	4144 Å	4250 Å	4260 Å	4272 Å
Fe I	4325 Å	4384 Å	4405 Å	4528 Å	4668 Å	4891 Å	4958 Å	5255 Å
Fe I	5269 Å	5616 Å	6609 Å	6663 Å	6678 Å			
Fe II	3914 Å	3938 Å	3945 Å	4179 Å	4233 Å	4385 Å		

Table 14: Various metals

Mg I	3838 Å	5167 Å	5137 Å	5184 Å			
Mg II	4481 Å						
Sc II	4247 Å						
Ti I	4523 Å	4527 Å	4533 Å	4545 Å	4617 Å		
Ti I	4640 Å	4982 Å	5036 Å	6258 Å			
Ti II	4164 Å	4300 Å	4395 Å	4400 Å	4408 Å	4444 Å	4468 Å
Cr I	4254 Å	4646 Å	4651 Å				
Cr II	4242 Å						
Mn I	3807 Å	4031 Å	4033 Å	4034 Å	4041 Å		
Sr II	4077 Å	4215 Å	4305 Å				
Sr III	4335 Å						
Eu II	4205 Å						

Table 15: Molecules

CH	CN	CN			
4300 Å	3883 Å	4216 Å			
TiO	TiO	TiO	TiO	TiO	TiO
4585 Å	4761 Å	4954 Å	5000 Å	5167 Å	6159 Å

Table 16: Emission lines in gaseous nebulae

O_I	O_I	O_I	O_I	O_{II}			
5007 Å	5577 Å	6300 Å	6363 Å	3727 Å			
O_{III}	O_{III}	O_{III}	O_{III}				
4363 Å	4391 Å	4959 Å	5007 Å				
Ne_{III}	S_{II}	Fe_{III}	N_I	Cl_{III}	Cl_{III}	N_{II}	S_{II}
3868 Å	4069 Å	4658 Å	5200 Å	5517 Å	5537 Å	5757 Å	6723 Å

Table 17: Earth atmosphere

O_2	O_2	O_2	O_2	O_2	H_2O
6280 Å	6867 Å	6875 Å	6906 Å	7594 Å	7165 Å